

2019

## A climatology of quasi-linear convective systems in the U.S.

Jacob Strohm

Follow this and additional works at: <https://huskiecommons.lib.niu.edu/allgraduate-thesesdissertations>

---

### Recommended Citation

Strohm, Jacob, "A climatology of quasi-linear convective systems in the U.S." (2019). *Graduate Research Theses & Dissertations*. 80.

<https://huskiecommons.lib.niu.edu/allgraduate-thesesdissertations/80>

This Dissertation/Thesis is brought to you for free and open access by the Graduate Research & Artistry at Huskie Commons. It has been accepted for inclusion in Graduate Research Theses & Dissertations by an authorized administrator of Huskie Commons. For more information, please contact [jschumacher@niu.edu](mailto:jschumacher@niu.edu).

## ABSTRACT

### A CLIMATOLOGY OF QUASI-LINEAR CONVECTIVE SYSTEMS IN THE U.S.

Jacob Strohm, M.S.  
Department of Geographic and Atmospheric Sciences  
Northern Illinois University, 2019  
Walker Ashley, Director

Quasi-linear convective systems, or QLCSs, are a common, organized thunderstorm mode in the U.S. Over the last fifty years, severe weather research has focused on the supercell, but recently QLCSs have become an increasingly important area of study. Researchers and operational meteorologists realize that this morphology is difficult to forecast and may be responsible for a large proportion of the severe weather reports in the eastern two-thirds of the U.S. This study seeks to determine the degree to which QLCSs threaten humans and their assets by first assessing their climatology and, second, measuring their contribution to the severe report record. Initially, an objective classification scheme was developed and employed to detect and track QLCSs on conterminous U.S. composite radar data spanning the most recent two decades. The objective classification scheme, or computer algorithm, was constructed using machine learning techniques on thousands of subjectively, expert-defined QLCSs from a sample of observed mesoscale convective system events during the observed record. After the scheme was tested and verified, a descriptive climatology of QLCSs was produced. The climatology assessed algorithm-identified QLCS slices (instantaneous footprint of an event) and swaths (the entire footprint of an event) as units of measure, providing the first long-term spatiotemporal analysis of this morphology. Thereafter, QLCS slices were linked with the severe storm database to determine the proportion of thunderstorm hazard reports produced by this

morphology. Results show that, on average, there are 139 QLCSs in any given year. The majority occur in three corridors, depending on the year and season: the eastern High Plains into western Missouri and Arkansas; the Midwest, stretching from Iowa through Wisconsin and northern Illinois to Indiana; and the South, from the central Gulf Coast to Tennessee. QLCSs are found to account for more than one-third of severe wind reports, as well as more than one-fifth of reported tornadoes. The overarching goal of the research was to 1) develop an objective analysis routine that can assist meteorologists in identifying QLCSs in observed and simulated radar reflectivity data, 2) provide the first objectively identified, long-term climatology of QLCSs in the U.S., and 3) increase scientific understanding of the impacts of QLCS hazards on the populace and built environment.

NORTHERN ILLINOIS UNIVERSITY  
DEKALB, ILLINOIS

MAY 2019

A CLIMATOLOGY OF QUASI-LINEAR CONVECTIVE SYSTEMS IN THE U.S.

BY

JACOB STROHM  
© 2019 Jacob Strohm

A THESIS SUBMITTED TO THE GRADUATE SCHOOL  
IN PARTIAL FULFILLMENT OF THE REQUIREMENTS  
FOR THE DEGREE  
MASTER OF SCIENCE

DEPARTMENT OF GEOGRAPHIC AND ATMOSPHERIC SCIENCES

Thesis Director:

Walker Ashley

## ACKNOWLEDGEMENTS

I would like to thank Dr. Walker Ashley for serving as my advisor for this project and providing continual support to make this thesis a success. Second, I owe a great deal of gratitude to Dr. Alex Haberlie, who assisted with the generation of data employed in this thesis. I would also like to thank my committee members, Drs. David Changnon and Zachary Handlos, for their input and advice throughout this process. Finally, I would like to thank the faculty and graduate students of the Geographic and Atmospheric Sciences Department, my friends, and my family, who all gave their insight and support when I needed a helping hand. This thesis would not have been completed without their help.

## TABLE OF CONTENTS

|                                    | Page |
|------------------------------------|------|
| LIST OF TABLES .....               | v    |
| LIST OF FIGURES .....              | vi   |
| Chapter                            |      |
| 1. INTRODUCTION .....              | 1    |
| Background .....                   | 2    |
| Hazards .....                      | 6    |
| 2. DATA AND METHODS .....          | 10   |
| Dataset.....                       | 10   |
| Methodology .....                  | 11   |
| 3. RESULTS .....                   | 16   |
| QLCS Climatology .....             | 16   |
| QLCS Storm Report Climatology..... | 40   |
| QLCS-attributable tornadoes .....  | 46   |

|                             |    |
|-----------------------------|----|
| QLCS-attributable wind..... | 51 |
| QLCS-attributable hail..... | 55 |
| 4. CONCLUSIONS.....         | 61 |
| REFERENCES .....            | 64 |

## LIST OF TABLES

| Table  | Page |
|--|------|
| 1. Definitions of QLCSs and linear MCSs employed in the contemporary literature .....                      | 5    |
| 2. QLCS counts and statistics for each month and year of the study period .....                            | 17   |
| 3. Counts of QLCS events for each year in each region, along with the total for all regions together. .... | 37   |

## LIST OF FIGURES

| Figure   | Page |
|--|------|
| 1. Sample QLCS event, with slice, swath, and storm report attributes.....  | 15   |
| 2. QLCS counts for each year between 1996 and 2017 .....   | 18   |
| 3. Cumulative QLCS counts for each month between 1996 and 2017 .....   | 18   |
| 4. Box and whisker plots displaying the difference in the number of QLCSs<br>observed during each month between 1996-2017. ....  | 20   |
| 5. Mean QLCS counts from 1996-2017 per hour for three-month periods .....  | 21   |
| 6. The annual mean distribution of QLCSs, with a white X marking the location<br>of the highest value .....                      | 23   |
| 7. Mean QLCS distribution for each month of the year, with the location of the<br>highest monthly mean marked by a white X ..... | 24   |
| 8. Total QLCS distribution for the years 1996-2017, with the location of the<br>highest annual total marked by a white X.....    | 28   |
| 9. Map depicting five chosen regions: the High Plains, Midwest, North Plains,<br>Northeast, and the South.....                   | 36   |
| 10. Mean QLCS counts per hour for five regions: the High Plains, Midwest,<br>North Plains, Northeast, and the South.....         | 38   |
| 11. Graphs of all hazards (wind, hail, tornado) for QLCS and non-QLCS<br>storms .....  | 41   |
| 12. As in Figure 11, but for tornado reports .....   | 47   |
| 13. As in Figure 12, but for severe wind reports .....   | 51   |
| 14. As in Figure 13, but for severe hail reports .....   | 56   |

## **1. Introduction**

Quasi-linear convective systems (QLCSs) are a subclassification of mesoscale convective systems (MCSs) and feature a convective line or line segments that are much longer than they are wide. QLCSs can include many organized system types such as squall lines, line echo wave patterns, and bow echoes. The QLCS mode has not been as widely studied as supercells, and the nature of QLCS severity and their propensity to threaten people and the built environment requires further investigation. Prior research has focused on a subset of QLCS types that produce distinct high-end hazards, such as derecho-producing convective systems (e.g., Corfidi et al. 2016, Guastini and Bosart 2016). Currently, no long-term climatological study of QLCSs exists. The purpose of this thesis was to develop and employ an automated QLCS classification system to investigate the spatiotemporal characteristics of QLCS and their hazards across the U.S. The fundamental research questions to be addressed in this work are:

1. How are QLCSs spatiotemporally distributed across the conterminous U.S.?
2. How do QLCSs vary spatiotemporally across the study period, and have they become more variable?
3. What proportion of observed severe and significant severe storm reports are attributable to the QLCS morphology, and how does this attribution vary spatiotemporally?

*a. Background*

QLCS research dates to the early 1980s, when the concept of the MCS was introduced, defined, and studied from a satellite-based perspective (Maddox 1980, Zipser 1982). MCS classification is difficult because expert identification is subjective, with varying definitions found in the literature (e.g., Gallus et al. 2008, Grams et al. 2012, Smith et al. 2012). Today, MCSs are generally defined by their radar characteristics and are considered assemblages of thunderstorms organized on a scale larger than their individual storm cells, where the cells act together to generate flows and features that provide overall system organization (Ashley et al. 2003). MCSs exist on the spatial and temporal scales of meso- $\alpha$  to meso- $\beta$ . Meso- $\alpha$  describes weather phenomena that range from 200km to 2000km in size and last several days to a week, whereas meso- $\beta$  describes weather phenomena that range from 20km to 200km in size and last several hours to a day (Orlanski 1975).

In the 1980s, satellite imagery was used as an objective means of classifying MCSs by their shape (Maddox 1980). Two proposed categories, at least initially, included large MCSs known as mesoscale convective complexes (MCCs), which are nearly circular, and persistent elongated convective systems (PECSs), which are nearly linear (Maddox 1980, Anderson and Arritt 1998, Jirak et al. 2003). These systems are identified using infrared satellite imagery, which aids in objectively categorizing the storms based on cloud top temperatures. For instance, MCCs must have a continuous cold cloud shield of  $\leq -32^{\circ}\text{C}$ , with an area  $\geq 100,000\text{km}^2$ , and their interior cold cloud region must be  $\leq -52^{\circ}\text{C}$ , with an area  $\geq 50,000\text{km}^2$ . These size definitions must be met for a minimum of 6 hours, and the size ratio between the minor and major axes must be  $\geq 0.7$  at the time of the system's maximum extent (Maddox 1980, Anderson

and Arritt 1998, Ashley et al. 2003). A PECS is a type of MCS that fulfills the infrared satellite-based definition of an MCC in every way except shape. PECSs have a minor to major axis ratio between 0.2 and 0.7, which results in them being more linear than MCCs (Anderson and Arritt 1998, Jirak et al. 2003).

MCSs, and in particular MCCs, occur most often during the night. As thunderstorms develop during the afternoon, they tend to increase in areal coverage into the overnight hours and dissipate the next day after sunrise (Maddox 1980, Velasco and Fritsch 1987, Miller and Fritsch 1991, Laing and Fritsch 1993a,b, Fritsch and Forbes 2001, Markowski and Richardson 2010, p. 266). MCCs favor the southern Great Plains during the spring but shift north during the summer months (Ashley et al. 2003). These storms are important because they contribute a significant amount of precipitation to the central U.S. during the warm season (Heideman and Fritsch 1984, Fritsch et al. 1986, Ashley et al. 2003, Jirak et al. 2003, Schumacher and Johnson 2006, Stevenson and Schumacher 2014, Campbell et al. 2017, Haberlie and Ashley 2019).

QLCSs are an important and unique subset of the MCS classification that has matured over decades of research, though definitions, which have largely been based on radar reflectivity imagery, have consistently been subjective and/or vague. During the 1980s, QLCSs were known largely as squall lines (Bluestein and Jain 1985). A squall line was defined as an MCS that was linearly oriented with less intense cells that have wind shifts and cool air outflow like the more intense cells of the line (Maddox 1980, Bluestein and Jain 1985). Squall lines were first classified into four types by their appearance on radar reflectivity by Bluestein and Jain (1985). Their development was described as either broken line, back building, broken areal, or embedded areal. Broken lines form when discrete cells develop in a line at approximately the same time, and as these cells expand, they congeal together into a continuous line. New cells may develop

in between the older ones, contributing to the solid line that eventually forms. Back-building lines experience new cell growth upstream of the old cells, relative to the system's motion. Over time, these cells merge, expanding the line. This process originates normally from a single cell but may occur with a group of widely spaced cells as well. Broken-areal formation is not quite as straightforward. It begins with an amorphous area of cells that have moderate or intense magnitudes. These cells combine as they grow upscale and form a continuous line of precipitation. Finally, embedded-areal formation is the least common. This subtype only occurs when a line of storms exists within a larger region of stratiform precipitation (Bluestein and Jain 1985). Broken line and back building were found to be the most common cases, at least across the study area of Oklahoma (Bluestein and Jain 1985, Jirak et al. 2003, Parker and Johnson 2000).

Though Bluestein and Jain (1985) is one of the most cited papers in the MCS literature, the manuscript did not provide explicit criteria for defining these systems but, as discussed, focused on their subjective identification and classification. The term "squall line" has now fallen generally out of favor and has been replaced by the more encompassing QLCS nomenclature, which was first introduced by Weisman and Davis (1998). That said, the extensive spectrum of observed MCSs and MCS subtypes makes "binning" and classifying these events difficult and time consuming. Indeed, even though there have been several decades of research on linear-oriented MCSs, the morphology has not been defined consistently in the literature, and there is a lack of dynamical underpinning to the definitions that do exist. Table 1 provides a sample of criteria used to define QLCSs in some of the contemporary literature, revealing both consistencies and variations in individual criteria employed.

Table 1. Definitions of QLCSs and linear MCSs employed in the contemporary literature. Events are typically defined using radar reflectivity thresholds, convective line length, length to width aspect ratio, and minimum amount of time that these criteria must be maintained.

| <b>Publication</b>        | <b>Min. Line Reflectivity</b> | <b>Length / Aspect Ratio</b> | <b>Min. Duration</b> |
|---------------------------|-------------------------------|------------------------------|----------------------|
| Parker and Johnson (2000) | > 40 dBZ                      | 100km / NA                   | 3h                   |
| Trapp et al. (2005)       | $\geq$ 40 dBZ                 | $\geq$ 100km / NA            | NA                   |
| Gallus et al. (2008)      | NA                            | $\geq$ 75km / 3 to 1         | 2h                   |
| Schoen and Ashley (2011)  | $\geq$ 40 dBZ                 | $\geq$ 75km / NA             | $\geq$ 30 minutes    |
| Grams et al. (2012)       | $\geq$ 40 dBZ                 | $\geq$ 100km / 3 to 1        | NA                   |
| Smith et al. (2012)       | $\geq$ 35 dBZ                 | $\geq$ 100km / 3 to 1        | NA                   |

Definitions also vary when considering whether cells in convective lines constitute QLCSs. When a QLCS begins to form, cells may develop simultaneously while still isolated from each other. Convective lines may result when these discrete cells combine and grow upscale. Over time, these cells fill in the precipitation-free spaces between them, developing a single cold pool and creating a solid line of convection (Bluestein and Jain 1985, Markowski and Richardson 2010, p. 245-248, Bluestein 2013, p.265-267). There are three different ways that the issue of contiguous reflectivity is addressed in the literature. First, contiguous reflectivity may be required over a certain horizontal distance, normally 75-100km (Gallus et al. 2008, Grams et al. 2012, Smith et al. 2012). Second, contiguous reflectivity may not be required, but cells must be within a certain distance from each other, or within a so-called buffer (Schoen and Ashley 2011). The third option is that contiguous reflectivity is not required at all, but the cells are arranged in a mostly linear fashion (Kis and Straka 2010).

Classification of QLCSs may also be done by examining the convective and stratiform regions of an MCS on radar to see how they are arranged (Parker and Johnson 2000, Jirak et al. 2003). Such an arrangement may take several different forms, including leading stratiform,

trailing stratiform, and parallel stratiform (Parker and Johnson 2000, Gallus et al. 2008, Duda and Gallus 2010, Houze 2018).

Recently, work was performed to classify MCSs objectively by their shape on radar reflectivity (Haberlie and Ashley 2018a,b). Tracking an MCS along its path involves two types of data: slices and swaths. Slices are the instantaneous footprints of a storm event at any given time; swaths are the entire footprint of the event throughout its full lifetime (Haberlie and Ashley 2018a,b). To distinguish between storm types, human (or so-called expert) “pattern recognition” is performed to categorize them based on visual appearance. In these cases, experts who research MCSs may classify morphologies on hundreds or even thousands of radar snapshots. This expert classification information is, in turn, used in a machine learning environment to formulate objective, computer-based algorithms for classifying data. These algorithms can be used to identify MCSs in tens of thousands of instantaneous radar depictions, removing the subjective and laborious activity required in the past by researchers (Haberlie and Ashley 2018a,b,c). However, to date, there has been limited work done to objectively identify MCS subtypes such as QLCSs in radar imagery using an algorithm.

*b. Hazards*

MCSs, including the QLCS archetype, can produce many different hazards, including floods, severe nontornadic winds and derechos, hail, and tornadoes (Fritsch et al. 1986, Johns and Hirt 1987, Doswell et al. 1996, Hilgendorf and Johnson 1998, Houze 2004, Ashley and Mote 2005, Gallus et al. 2008, Campbell et al. 2017). Widespread and flash flooding from these storms pose a great threat to life (Ashley and Ashley 2008). The structure and arrangement of precipitation in any MCS are crucial in determining how much flooding will occur (Doswell et

al. 1996, Parker and Johnson 2000, Schumacher and Johnson 2005). Some MCSs can exhibit a “training” pattern, whereby cells repetitively form and pass over the same location, leading to flash flooding. In other cases, MCSs themselves form repeatedly over several days and pass over the same location (Doswell et al. 1996, Pettet and Johnson 2003, Schumacher and Johnson 2005), leading to widespread flooding (Doswell et al. 1996). Because of these characteristics, MCSs may be responsible for as much as 40% of the deaths that result from flooding in the U.S. (Ashley and Ashley 2008).

Severe winds from both tornadic and nontornadic storms are the most serious threat to people’s lives and property. Organized linear storms were found to be responsible for 42% of fatalities from nontornadic convective winds between 1998 and 2007 (Schoen and Ashley 2011). The greatest threat of nontornadic high winds comes from a QLCS subtype known as the bow echo (Fujita 1978); this storm morphology has a tendency to produce progressive derechos, which can have devastating socioeconomic impacts (Ashley and Mote 2005, Schoen and Ashley 2011). Warm-season derechos (May through August) have been found to occur in two main corridors: one across the Midwest from Minnesota to Ohio and another in the Southern Plains, centered near Oklahoma, Kansas, and Missouri (Johns and Hirt 1987, Bentley and Mote 1998, Congilio and Stensrud 2004, Ashley and Mote 2005, Guastini and Bosart 2016). Because bow echoes produce such strong winds, this distribution somewhat mirrors that of QLCS significant severe wind reports (Smith et al. 2012). During the warm season, reports are most frequent in the Midwest, from Iowa to Indiana. During the spring, reports are not clustered in common derecho corridors, instead favoring the American South, including Kentucky, Tennessee, and Mississippi (Smith et al. 2012). Gallus et al. (2008) found that, of nine storm morphologies (five linear, three cellular, one nonlinear), bow echoes had nearly twice as many reports of

nontornadic severe wind than the next morphology. The top four storm modes for severe wind greater than 65 kt were all linear systems: bow echo, trailing stratiform, parallel stratiform, and leading stratiform (Gallus et al. 2008).

Tornadoes are another hazard that can be produced by MCSs and QLCSs. They are not as frequent in this storm mode as they are with supercells but still present numerous dangers to the public due to their forecast difficulty. Over a three-year period, Trapp et al. (2005) showed that cells produced about 79% of tornadoes while QLCSs produced about 18%. Furthermore, QLCS tornadoes may produce 35% to 50% of all tornadoes in the Midwest (Trapp et al. 2005, Grams et al. 2012), with many of these tornadoes forming from processes that are different from, and more difficult to detect compared to, mesocyclones in supercells (Trapp and Weisman 2003, Atkins and St. Laurent 2009). Smith et al. (2012) found a similar distribution, with up to 40% of Midwest tornadoes associated with linear MCSs. Most of these occur during the spring, with a maximum around Illinois, Indiana, and Kentucky (Smith et al. 2012). Normally, these tornadoes are weaker than those from discrete cells or supercells, but they also form during the night more often than cellular tornadoes (Trapp et al. 2005, Kis and Straka 2010, Skow and Cogil 2017). Nocturnal tornadoes are more dangerous than those during the day because they are more difficult to identify, warnings are less likely to be received while people are sleeping, and they strike when people are in more vulnerable housing structures (Ashley et al. 2008, Black and Ashley 2011). Brotzge et al. (2013) found that the probability of detection (POD) of supercells was 85.4% compared to 45.8% for nonsupercells, which included QLCSs and other, disorganized modes. Though QLCS tornadoes have a propensity to occur at night (Trapp et al. 2005, Kis and Straka 2010, Skow and Cogil 2017) and be difficult to warn, 97% of tornado fatalities and 92% of damage resulted from supercells and not QLCSs (Brotzge et al. 2013). Yet

again, the key difference was supercells in lines; they had nearly twice the fatalities and more than 2.5 times the injury rate per tornado than other supercells.

## 2. Data and Methods

### *a. Dataset*

This study uses quality-controlled, NOWrad composites of WSR-88D radar data. NOWrad data have a spatial resolution of 2 km x 2 km and a temporal resolution of 5 and 15 minutes. Reflectivity values are displayed in intervals of 5 dBZ (Parker and Knievel 2005). These data are the basis for identifying and tracking the QLCSs using the algorithm.

The contribution of severe storm reports by QLCSs was assessed by using the SVRGIS dataset maintained by the Storm Prediction Center (SPC) at <http://www.spc.noaa.gov/gis/svrgis/>. The SVRGIS dataset includes dozens of variables such as the start and end latitudes/longitudes (times) of each report, the report type, and casualty count. As with any data, there are limitations to the severe storm report databases. Storm reports may come from trained spotters or from the public. Magnitudes of the reported hazards cannot always be verified and are often estimated through damage surveys. In the case of wind speeds, this may lead to overestimation of actual values (Trapp et al. 2006, Smith et al. 2013, Edwards et al. 2018). Additionally, sharp discontinuities are found in the convective gust reports across National Weather Service county warning areas (Doswell et al. 2005, Edwards et al. 2018). Reports are also dependent on population density and time of day (Doswell and Burgess 1988, Trapp et al. 2006, Smith et al. 2013, Campbell et al. 2017). The ratio of estimated gusts to measured gusts varies across the U.S., and measured gusts cluster around population centers (Edwards et al. 2018). Although these errors are known to exist, this study did not seek to adjust the SVRGIS dataset to account for these biases. Some storm reports were found to have no parent storm nearby (i.e., possible

error in time of storm report), as evidenced from a lack of radar reflectivity in the area. These storm reports were filtered out of the dataset to avoid including reports that were not associated with a QLCS.

*b. Methodology*

This study employs the Parker and Johnson (2000) MCS definition as the foundation for developing an algorithm that can objectively classify QLCSs. Parker and Johnson state that a linear MCS contains a convective line with contiguous or nearly contiguous chains of convective echoes that share a common leading edge. Whether they are arranged nearly in a straight line or a slight curve, these echoes move in tandem (Parker and Johnson 2000). Only lines of convection, which are typically defined as echoes  $\geq 40$  dBZ in reflectivity (Trapp et al. 2005, Schoen and Ashley 2011), that extend 100 km or more and last a minimum of two hours will be considered in this research. QLCSs are also required to have a major axis length that is three times greater than their minor axis length, which, again, is consistent with the literature (Gallus et al. 2008, Schoen and Ashley 2011, Grams et al. 2012, Smith et al. 2012).

The MCS classification and tracking algorithm described by Haberlie and Ashley (2018a,b,c) was applied to QLCSs using an expert classification of thousands of MCS slices, which were binned in one of three types: QLCS, non-QLCS, or “maybe” QLCS. This expert classification was informed based on the QLCS definitional considerations discussed above. Two experts—Drs. Walker Ashley and Alex Haberlie—individually classified a sample of 3000 random slices and then compared their results to develop consistent QLCS and non-QLCS samples. One thousand eighty-seven QLCS slices were subjectively identified, along with 1,835 non-QLCS slices. About 80% of these slices were used to inform a machine learning algorithm

in objectively detecting QLCS slices compared to a sample of these events that met the experts' subjective QLCS classification. The model is trained by extracting pixels in a 256 x 256 km region centered on the most intense portion of a slice (Gagne et al. 2017). Next, data augmentation (Krizhevsky et al. 2012, Dieleman et al. 2015) is performed with the training data by randomly rotating each image by  $\pm 20$  degrees and randomly scaling the height and width of each image by  $\pm 20\%$ . This helps to prevent the algorithm from memorizing the training data and overfitting slices. By randomly changing the images, the structure of the storm itself as well as its rainfall intensity are emphasized over its size and orientation. With these data, the model correctly categorized 370 of 387 non-QLCS slices, or 96%, and 172 of 198 QLCS slices, or 87%. This indicates the model may have somewhat undercounted QLCSs, as 9% of non-QLCS slices were labelled as QLCSs, but 13% of QLCS slices were labelled as non-QLCSs. The algorithm was found to produce reasonable results, as samples with a QLCS probability of  $\geq 0.95$  tended to contain linear structures while samples with a QLCS probability of  $\leq 0.05$  were generally non-linear MCS structures.

This informed algorithm was applied to a 22-year dataset (1996-2017) consisting of conterminous U.S. (CONUS) composite radar reflectivity data, or NOWrad, as described. This process of "supervised classification" improves the overall effectiveness of the algorithm (Haberlie and Ashley 2018a,b,c). MCSs were identified through the following steps: Convective cells ( $\geq 40$  dBZ) with intense rainfall echoes  $\geq 50$  dBZ were identified and then aggregated into regions to separate them from convective systems in other areas of the U.S. These regions were based on a 24km search radius, and connected regions with a major axis  $\geq 100$  km in length are part of stratiform precipitation regions ( $\geq 20$  dBZ). Stratiform regions are located within a radius of 96 km, and identification of these convective cells and connected

stratiform regions makes up a slice. Each slice is then assigned an MCS probability using an ensemble machine learning classifier. The MCS slices are combined into swaths by examining whether they overlap both spatially and temporally. To choose the swaths most likely to be MCSs, a probability of 0.95 is required, and any slices that are below this confidence level are not included when constructing the swaths. If an MCS meets this threshold, it is tracked over its lifespan as long as it maintains a probability above 0.5. After creating the swaths, only those that last a minimum of three hours (Parker and Johnson 2000) are counted as MCS swaths.

Within this MCS dataset, QLCSs are distinguished from non-QLCSs using the image classification algorithm. The algorithm assigns a probability to each slice that ranges from 0 (very likely a non-QLCS) to 1 (very likely a QLCS). Within an MCS swath, a QLCS is identified if the swath's major axis maintains a 3 to 1 ratio for at least 2 hours. Over the lifetime of each QLCS, radar slices were concatenated to create QLCS event swaths. These swaths reveal the entire area, or footprint, covered by the QLCS from initiation to termination. Initiation occurs at the time when the QLCS meets the minimum length and reflectivity thresholds of 100km and 40 dBZ, respectively. Termination occurs when the QLCS no longer meets these requirements.

Using the slice and swath data, a descriptive climatology of QLCSs was created. The primary maps show frequency of QLCS occurrence and spatial patterns by overlapping swaths in a gridded framework, which was performed by counting the frequency of each event or unit of analysis in each polygon. Maps of various spatiotemporal attributes were supplemented by graphs and tables showing descriptive statistics of QLCS frequencies and other pertinent characteristics.

After the climatology was constructed, the QLCS dataset was then merged with the SVRGIS dataset. Each storm report was matched to the corresponding algorithm-identified QLCS radar slice in *ArcMap*. To do this, storm reports were selected for each 15-minute interval closest to an algorithm-identified slice. Reports that occurred at the same time but were not associated with the QLCS slice were eliminated by performing a “clip” of the data in the storm report layer in 15-minute intervals with the corresponding QLCS slice layer. As an example, if a report occurs at 0222Z, it will be associated with the slice that encompasses the time closest to it at 0215Z. To create the swath, a “merge” was performed on the slices to create a single shapefile that combines them all. Next, the “dissolve” tool was used to eliminate the internal boundaries of the slices. What remains is the footprint of the QLCS over its lifetime, or the swath. By eliminating storm reports outside the boundaries of each slice, only those storm reports produced by the QLCS lie within the swath (Figure 1). To scale up this analysis and apply it to every case in the dataset, a Python script was used to automate the *ArcMap* methodology, using the logic discussed.

A small 20km buffer was applied to the QLCS slices to capture storm reports caused by possible storm outflows (i.e., in some cases, severe winds can extend in advance of radar returns affiliated with a radar-defined QLCS). The buffer was carefully evaluated to avoid inaccurately capturing nearby supercells or other isolated convection not affiliated with the QLCS. This could artificially inflate the number of severe storm reports attributable to QLCS. A review of 69 radar images with buffers of 10km, 20km, 50km, and 100km revealed that the 20km buffer was the most efficient at capturing QLCS-affiliated storm reports and reducing false positives/negatives.

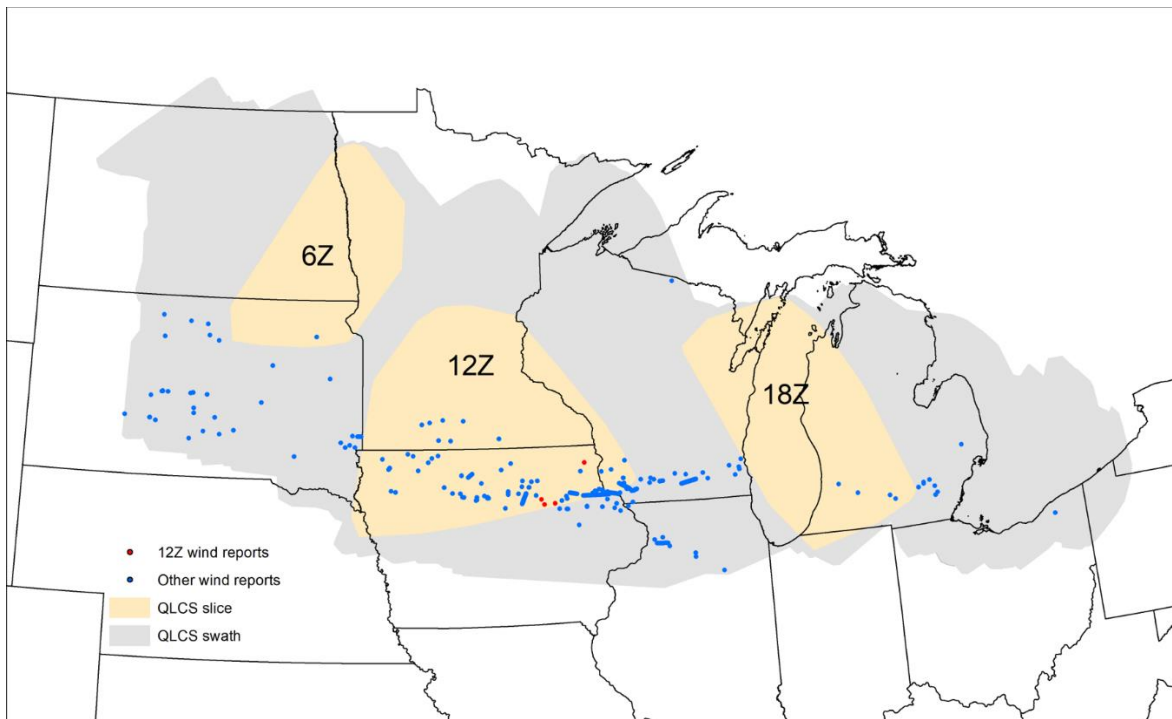


Figure 1. Sample QLCS event, with slice, swath, and storm report attributes. The beige polygons represent QLCS slices at 6Z, 12Z, and 18Z on 22 June 2015. The gray shading represents the full swath covered by the QLCS. The blue dots show severe wind reports within the swath. Multiple slices can and do overlap spatially (but not temporally), so not all wind reports shown in the three slices (6Z, 12Z, and 18Z) are part of corresponding slices. For example, only the red dots (12Z wind reports) are temporally part of the 12Z slice.

A variety of spatiotemporal climatologies of QLCS-attributed severe reports are assessed and represented using maps and charts. Further, the proportion of severe hazard reports due to QLCSs is provided. Together, these research products provide a new perspective on the propensity of QLCSs to produce severe hazards and the nature of the hazards themselves.

### **3. Results**

#### *a. QLCS Climatology*

From 1996 and 2017, 3,064 QLCS events were identified across the eastern two-thirds of the CONUS, equating to a mean (median) of 139 (138) per year. Similar to MCSs (Haberlie and Ashley 2019) and other convective phenomena (Ashley et al. 2003), the annual frequency of these storms was highly variable with a high of 182 in 2008 and a low of 101 in 1999 (Table 2, Figure 2). Although a regression analysis shows a slight increase of 0.5 QLCSs per year during the period of record, no clear trend is evident in Figure 2.

Overall, the frequency of QLCSs increases appreciably beginning in March and peaks during the warm-season in June. This is not the case every year, as 10 out of 22 years see the greatest QLCS activity in May instead of June. The latter part of the warm-season—July and August—have fewer QLCS counts than May and June, which may be a result of reduced baroclinity and a northward shift in extratropical cyclone tracks that occurs during the latter part of the warm-season (Eichler and Higgins 2006). MCCs have also been found to decrease in numbers, relative to their peak, during the end of the warm-season and early transition-season, which indicates that QLCSs are not unique among the MCS family when it comes to seasonal trends (Ashley et al. 2003). The number of QLCSs drops by 33% from June to July, and continues a downward trend until the annual minimum in December (Figure 3). Each month varies differently in the amount of QLCS experienced, but, in general, this variability increases

Table 2. QLCS counts and statistics for each month and year of the study period.

|                   | Jan  | Feb  | Mar  | Apr   | May   | Jun   | July  | Aug   | Sep  | Oct  | Nov  | Dec  | Annual Total |
|-------------------|------|------|------|-------|-------|-------|-------|-------|------|------|------|------|--------------|
| 1996              | 5    | 6    | 12   | 15    | 29    | 21    | 18    | 11    | 11   | 8    | 5    | 6    | 147          |
| 1997              | 6    | 1    | 10   | 15    | 26    | 30    | 12    | 9     | 3    | 5    | 5    | 1    | 123          |
| 1998              | 9    | 11   | 14   | 10    | 18    | 37    | 19    | 8     | 13   | 7    | 3    | 2    | 151          |
| 1999              | 6    | 3    | 6    | 9     | 24    | 20    | 13    | 11    | 4    | 5    | 0    | 1    | 102          |
| 2000              | 3    | 8    | 11   | 13    | 30    | 28    | 17    | 17    | 10   | 6    | 4    | 0    | 147          |
| 2001              | 2    | 2    | 10   | 3     | 23    | 20    | 18    | 16    | 13   | 9    | 4    | 3    | 123          |
| 2002              | 1    | 1    | 10   | 12    | 24    | 24    | 14    | 21    | 6    | 8    | 5    | 7    | 133          |
| 2003              | 2    | 4    | 12   | 6     | 21    | 38    | 25    | 6     | 9    | 2    | 6    | 2    | 133          |
| 2004              | 3    | 5    | 7    | 17    | 36    | 36    | 23    | 14    | 6    | 8    | 2    | 1    | 158          |
| 2005              | 3    | 3    | 7    | 12    | 23    | 38    | 20    | 9     | 12   | 2    | 6    | 2    | 137          |
| 2006              | 6    | 6    | 8    | 15    | 24    | 19    | 16    | 13    | 9    | 7    | 6    | 2    | 131          |
| 2007              | 2    | 3    | 16   | 11    | 21    | 22    | 16    | 26    | 4    | 12   | 5    | 5    | 143          |
| 2008              | 6    | 9    | 9    | 19    | 26    | 41    | 29    | 19    | 5    | 5    | 8    | 6    | 182          |
| 2009              | 2    | 8    | 9    | 24    | 21    | 26    | 21    | 28    | 4    | 11   | 1    | 5    | 160          |
| 2010              | 3    | 6    | 10   | 14    | 25    | 37    | 19    | 26    | 18   | 6    | 6    | 3    | 173          |
| 2011              | 6    | 4    | 12   | 24    | 26    | 30    | 16    | 20    | 11   | 6    | 7    | 1    | 163          |
| 2012              | 5    | 9    | 10   | 11    | 20    | 16    | 15    | 9     | 9    | 5    | 2    | 6    | 117          |
| 2013              | 7    | 2    | 6    | 12    | 31    | 26    | 8     | 12    | 4    | 5    | 2    | 2    | 117          |
| 2014              | 1    | 3    | 4    | 14    | 15    | 33    | 17    | 10    | 12   | 8    | 3    | 2    | 122          |
| 2015              | 2    | 2    | 1    | 18    | 26    | 19    | 17    | 12    | 5    | 4    | 7    | 5    | 118          |
| 2016              | 3    | 4    | 14   | 21    | 30    | 24    | 29    | 13    | 15   | 3    | 8    | 6    | 170          |
| 2017              | 8    | 10   | 12   | 22    | 24    | 22    | 22    | 11    | 3    | 6    | 5    | 4    | 149          |
| Monthly Total     | 91   | 110  | 210  | 317   | 543   | 607   | 404   | 321   | 186  | 138  | 100  | 72   |              |
| Monthly Mean      | 4.14 | 5.00 | 9.55 | 14.41 | 24.68 | 27.59 | 18.36 | 14.59 | 8.45 | 6.27 | 4.55 | 3.27 |              |
| Monthly Median    | 3    | 4    | 10   | 14    | 24    | 26    | 17.5  | 12.5  | 9    | 6    | 5    | 2.5  |              |
| Monthly Std. Dev. | 2.28 | 2.95 | 3.39 | 5.31  | 4.57  | 7.44  | 4.98  | 6.13  | 4.22 | 2.49 | 2.17 | 2.07 |              |
| CV                | 0.55 | 0.59 | 0.35 | 0.37  | 0.19  | 0.27  | 0.27  | 0.42  | 0.5  | 0.4  | 0.48 | 0.63 |              |

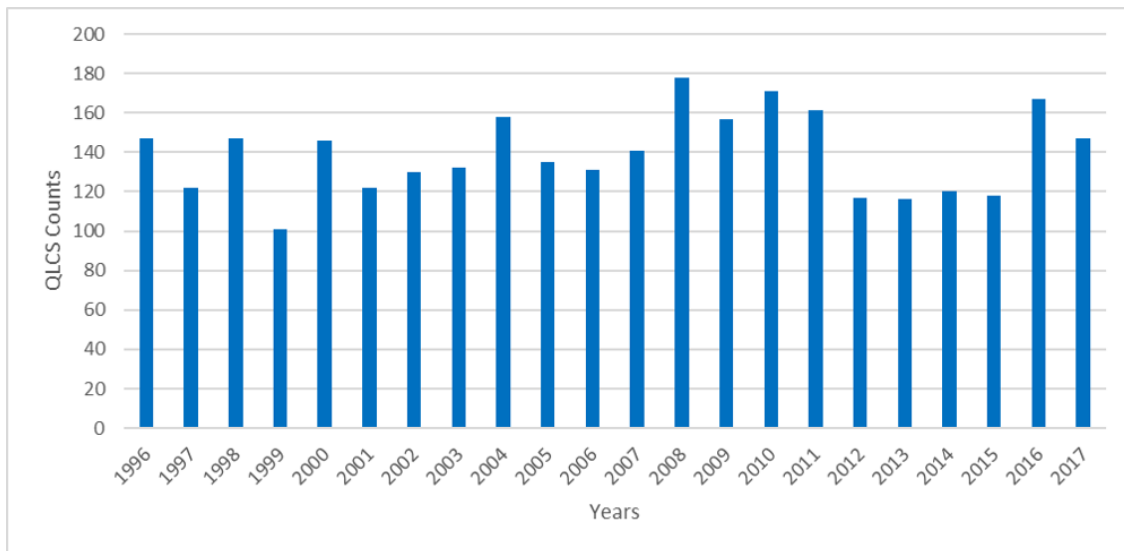


Figure 2. QLCS counts for each year from 1996 to 2017.

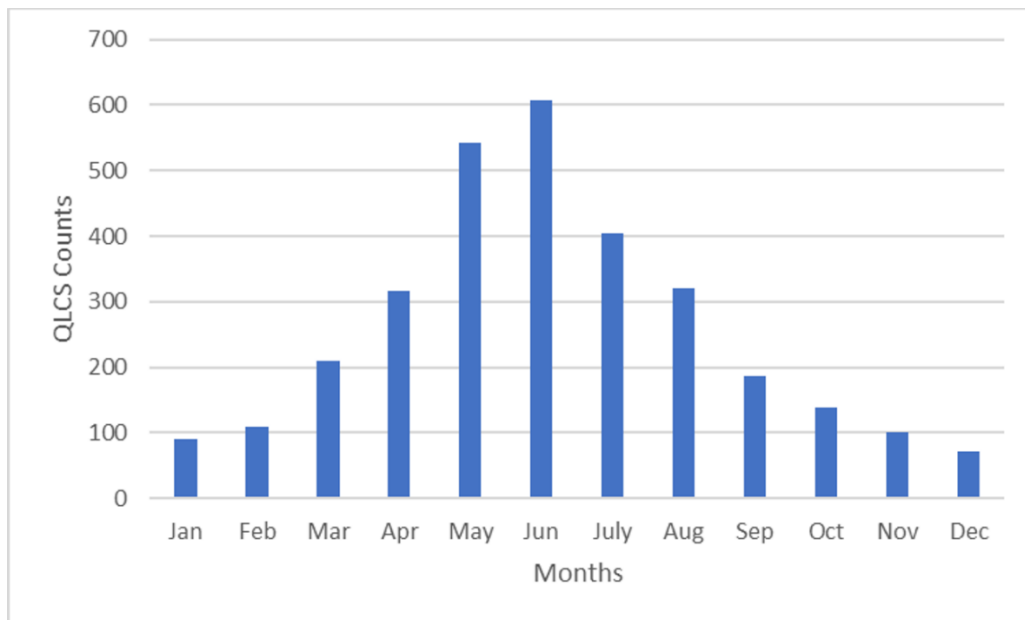


Figure 3. Cumulative QLCS counts for each month between 1996 and 2017.

during the warm-season. However, the greatest variation from the mean is seen in the fall and winter months.

There is a sharp transition between April and May, during which the minimum number of QLCSs observed rises above the mean of any previous month of the year. This may be due to an increase in convective available potential energy (CAPE) in the atmosphere, as well as a poleward shift in the region of maximum baroclinity, combined with linear forcing mechanisms generated by mid-latitude cyclones that are more common in transition seasons (Ashley et al 2003, Eichler and Higgins 2006, Gensini and Ashley 2011). QLCSs typically peak in June, though the observed number of storms varies annually by up to 25 events during this month. Although June and July are both in the midst of the warm season, they are notably different in terms of QLCS development. This discrepancy is not seen in MCSs as a whole (Haberlie and Ashley 2019), which occur at a steady rate from June to August. MCSs are able to form due to high CAPE values present in the eastern Great Plains and Mississippi Valley during the summer (Gensini and Ashley 2011), but decreased extratropical cyclone activity removes the linear forcing mechanisms supportive of QLCS formation (Ashley et al. 2003). The sudden shift in activity, similar to that between April and May, splits the warm season into two parts. Such distinct patterns are not found after the transition to the cool-season, when each month becomes much more similar to the next and QLCS activity drops (Figure 4).

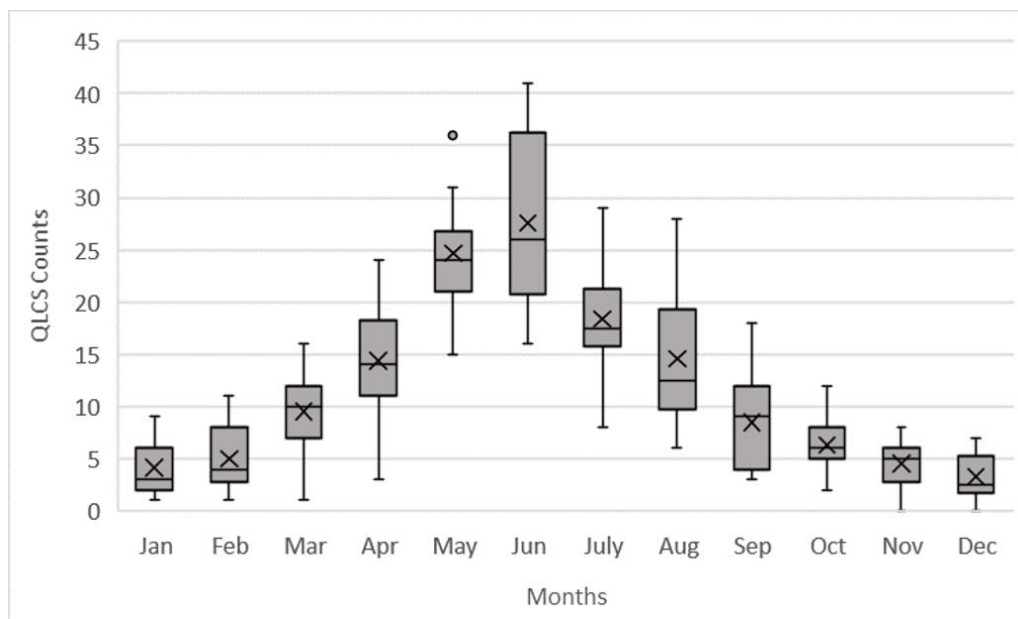


Figure 4. Box and whisker plots displaying the difference in the number of QLCSs observed during each month between 1996-2017. The interquartile range is represented by the shaded box, within which the mean is marked by an X and the median with a solid line. Whiskers extend to the 10<sup>th</sup> and 90<sup>th</sup> percentiles, and a single outlier exists in the data, shown with a circle in the plot for May.

As in prior assessments of MCSs (Jirak et al. 2003, Trapp et al. 2005, Schumacher and Johnson 2006, Haberlie and Ashley 2019), QLCSs exhibit diurnal patterns (Figure 5). During the warm-season, QLCSs favor the afternoon and nighttime hours. Overall, the highest number of QLCSs is experienced at night from 05 to 06Z. Their frequency decreases throughout the day, reaching a minimum around 17 to 18Z. At this minimum, QLCSs are less than half as frequent than they are at their nocturnal peak. These diurnal patterns are most noticeable during the transition-season months of MAM and warm-season months of JJA. Both of these monthly periods observe maximum (minimum) QLCS counts from 04 to 05Z (16 to 17Z). Although JJA has the highest mean QLCS count of any season during the early morning hours, these warm-season months have fewer QLCSs than MAM from the late morning to late afternoon hours.

The QLCS diurnal cycle is dampened during the fall transition and cool seasons (Figure 5). QLCSs during these seasons are less likely to be driven by cold pool dynamics and the low-level jet; rather, their forcing tends to be affiliated with migratory extratropical cyclones that have no preferential diurnal signal.

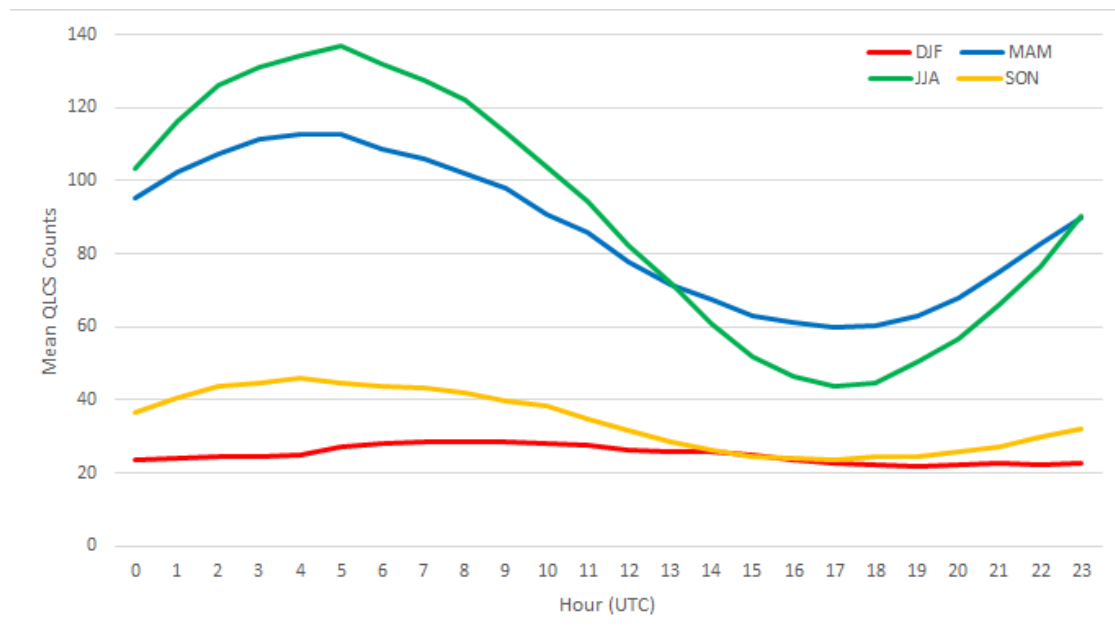


Figure 5. Mean QLCS counts from 1996-2017 per hour for three-month periods.

The spatial distribution of QLCSs varies widely across the eastern two-thirds of the U.S. (Figure 6). Most QLCSs occur east of the Continental Divide, with broad maxima occurring in the eastern Great Plains and Ozark Plateau, as well as the central Mississippi, lower Ohio, and Tennessee River Valleys. In the maxima, there are roughly 13 to 16 QLCSs that occur per year; surrounding these areas, a large region of the eastern CONUS—including the Midwest and Southeast—experiences as many as 10 to 13 QLCSs per year (Figure 6). This broad distribution shows some similarities to the assessment of various classifications of linear convection,

including QLCSs, in Smith et al. (2012). The Smith et al. research and results from this study both display a corridor of high QLCS activity from southern Illinois and Indiana stretching into Mississippi and Alabama. However, Smith et al. (2012) does not display a second maximum in QLCS activity in the eastern Great Plains, apart from a small area of increased QLCS significant wind events during the summer months. This maximum in the Great Plains must not be overlooked, as this study finds it is the location of the highest annual mean QLCS activity, with over 16 storms per year in extreme southeastern Kansas (Figure 6). The discrepancy between Smith et al. and the results herein is likely due to Smith et al.'s assigning of storm morphology based on significant severe storm reports in a 40 km grid rather than a storm-specific morphology climatology facilitated here, as well as notable differences in the periods of record.

During the cool season, QLCS activity is clustered in the Southeast, with a seasonal maximum located consistently in Alabama (Figure 7a-c). As the spring transition season arrives, the climatological pattern becomes much more dynamic, with a near doubling of monthly QLCS rates from January through April and an expanding area affected by QLCSs. The center of maximum QLCS activity grows and shifts northwestward in April, with event frequencies of two to three per month encompassing Mississippi, Arkansas, and portions of Tennessee and Kentucky. Activity in the Midwest and southern Plains is more frequent in April, with most areas in these regions experiencing one to two QLCSs per month (Figure 7d). Late spring continues the climatological trend in northwestward progression of QLCSs, with maximum activity in May located in the eastern Kansas, Oklahoma, and western Missouri. These areas experience, on average, three to four QLCSs in May, and this high monthly QLCS count increases in spatial coverage into Iowa during June. Despite this spatial increase in QLCS risk, the absolute maximum remains in Kansas in May and June (Figure 7e-f).

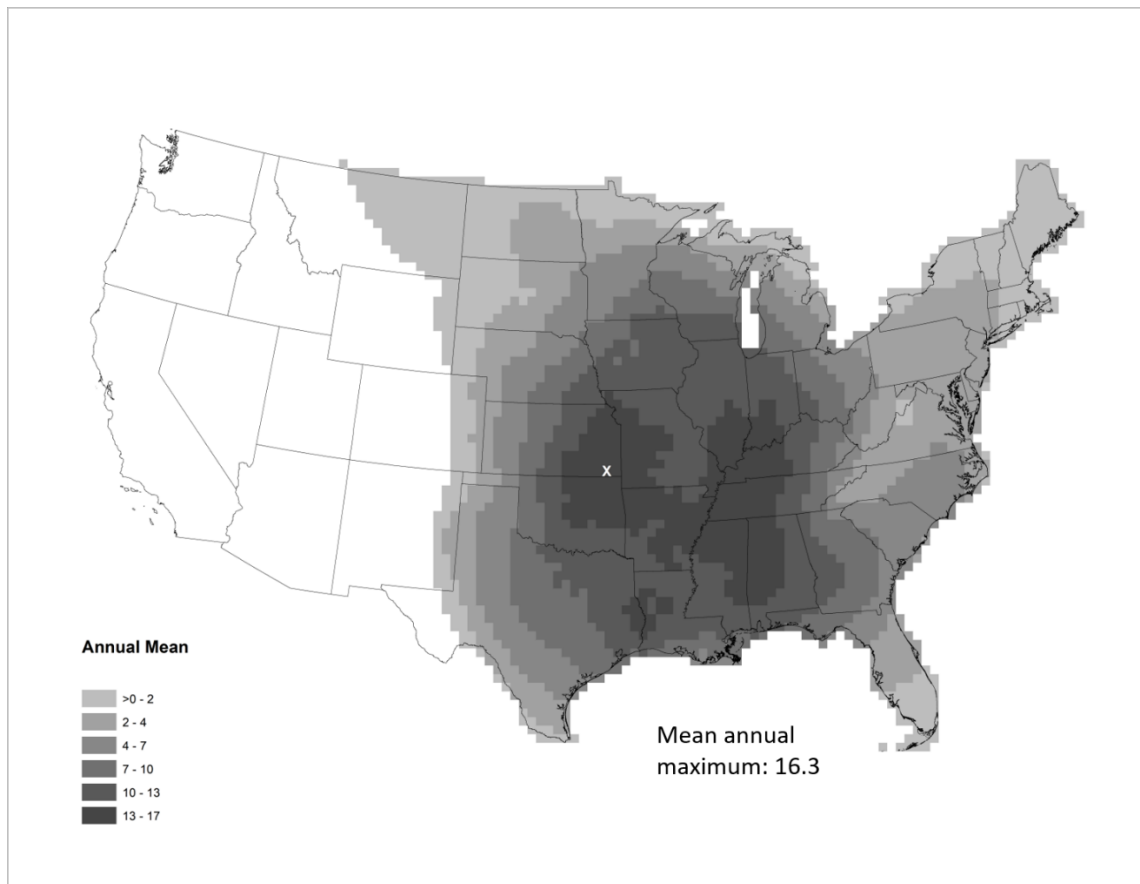


Figure 6. The annual mean distribution of QLCSs, with a white X marking the location of the highest value.

The pattern shifts as summer begins, and, in July and August, QLCSs are centered over the Upper Midwest. This notable spatial change is accompanied by a 33% month-over-month drop in QLCS frequencies after the June peak. Accordingly, the highest rate of QLCS occurrence in active corridors in both July and August is two to three per month, with a high-frequency corridor centered over the Corn Belt (Figure 7 g-h). This spatiotemporal distribution is similar to the long-term, progressive derecho climatology revealed by Guastini and Bosart (2016), suggesting that many of the QLCSs in this warm-season corridor may be affiliated with

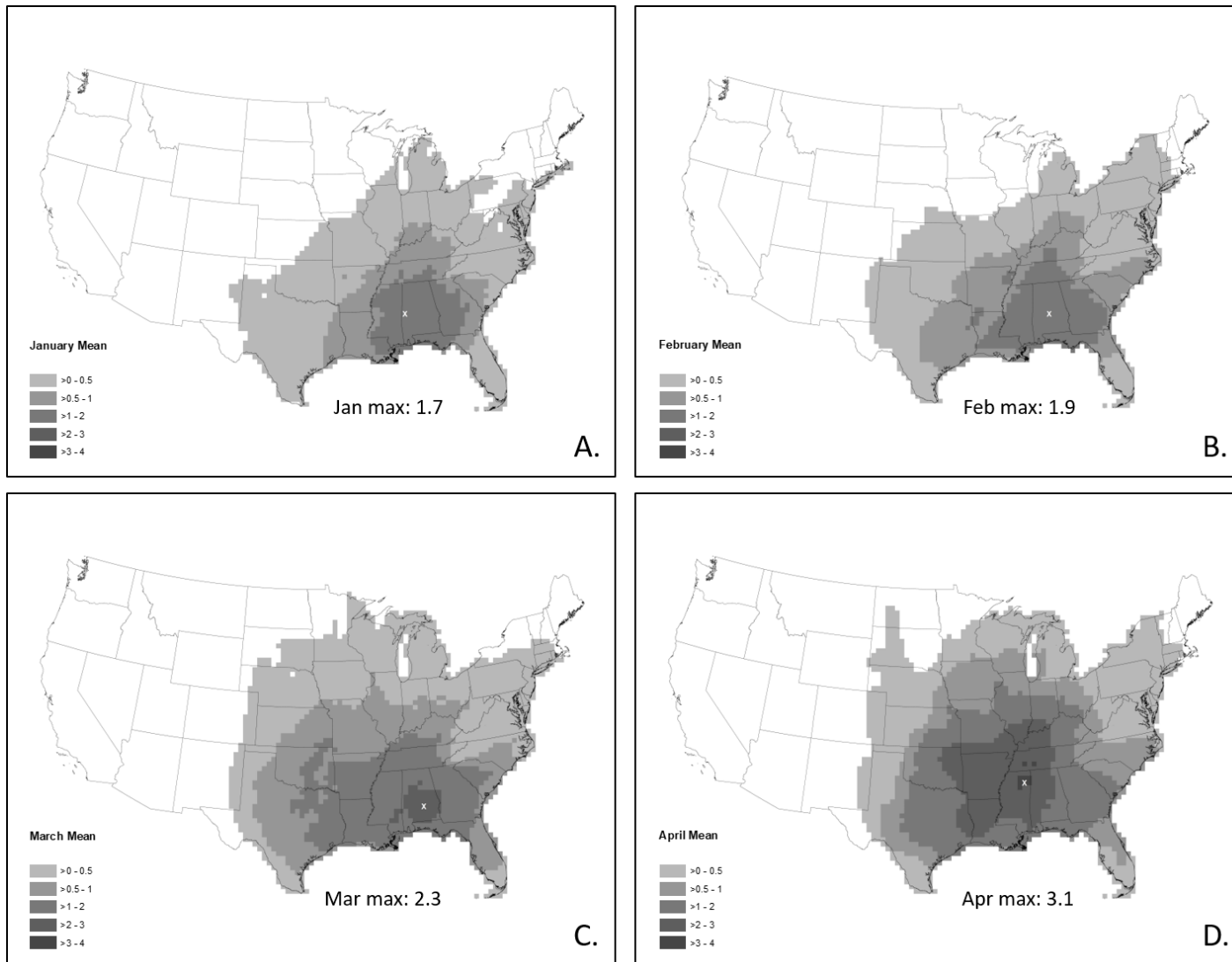


Figure 7. Mean QLCS distribution for each month of the year, with the location of the highest monthly mean marked by a white X.

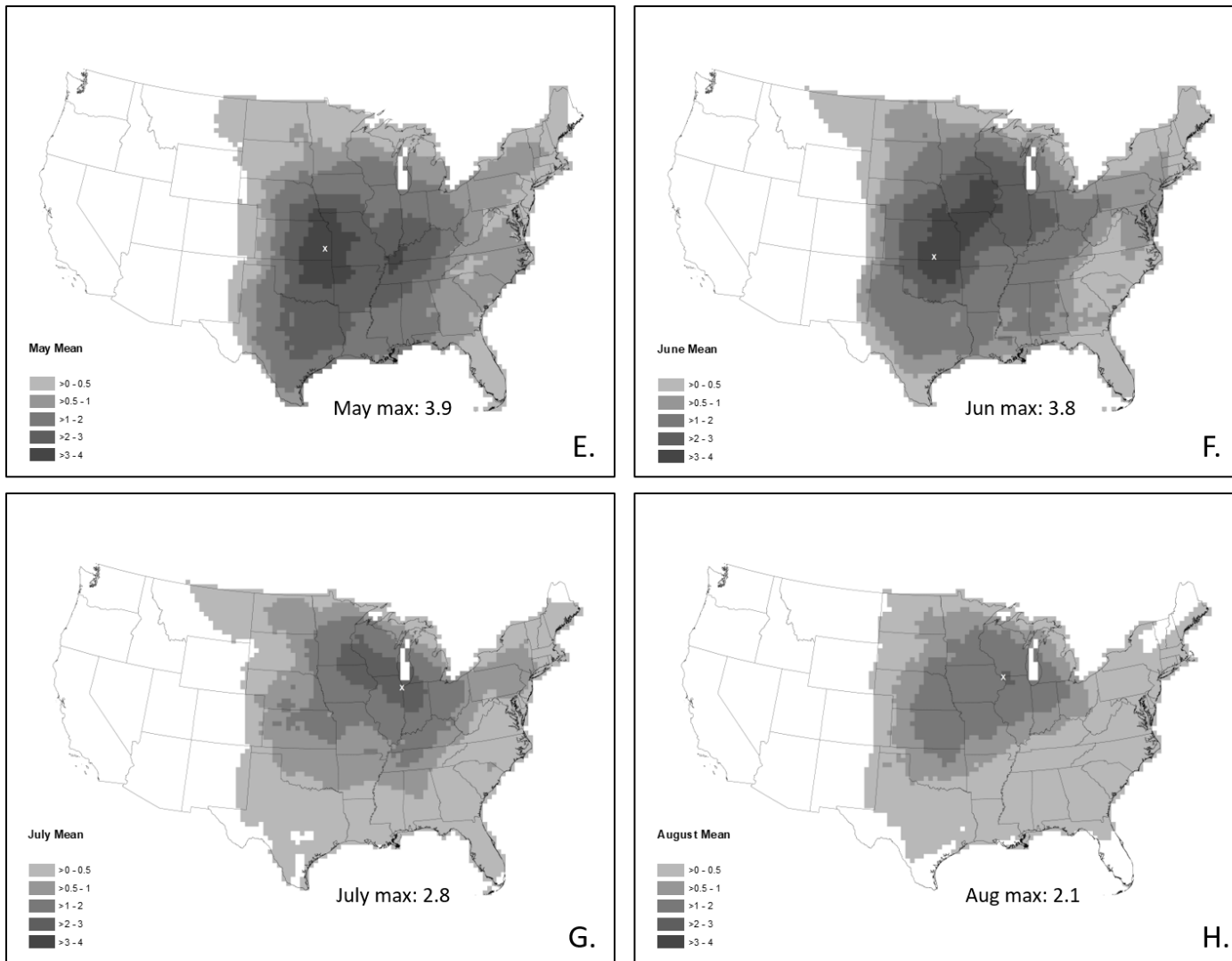


Figure 7. Continued on following page.

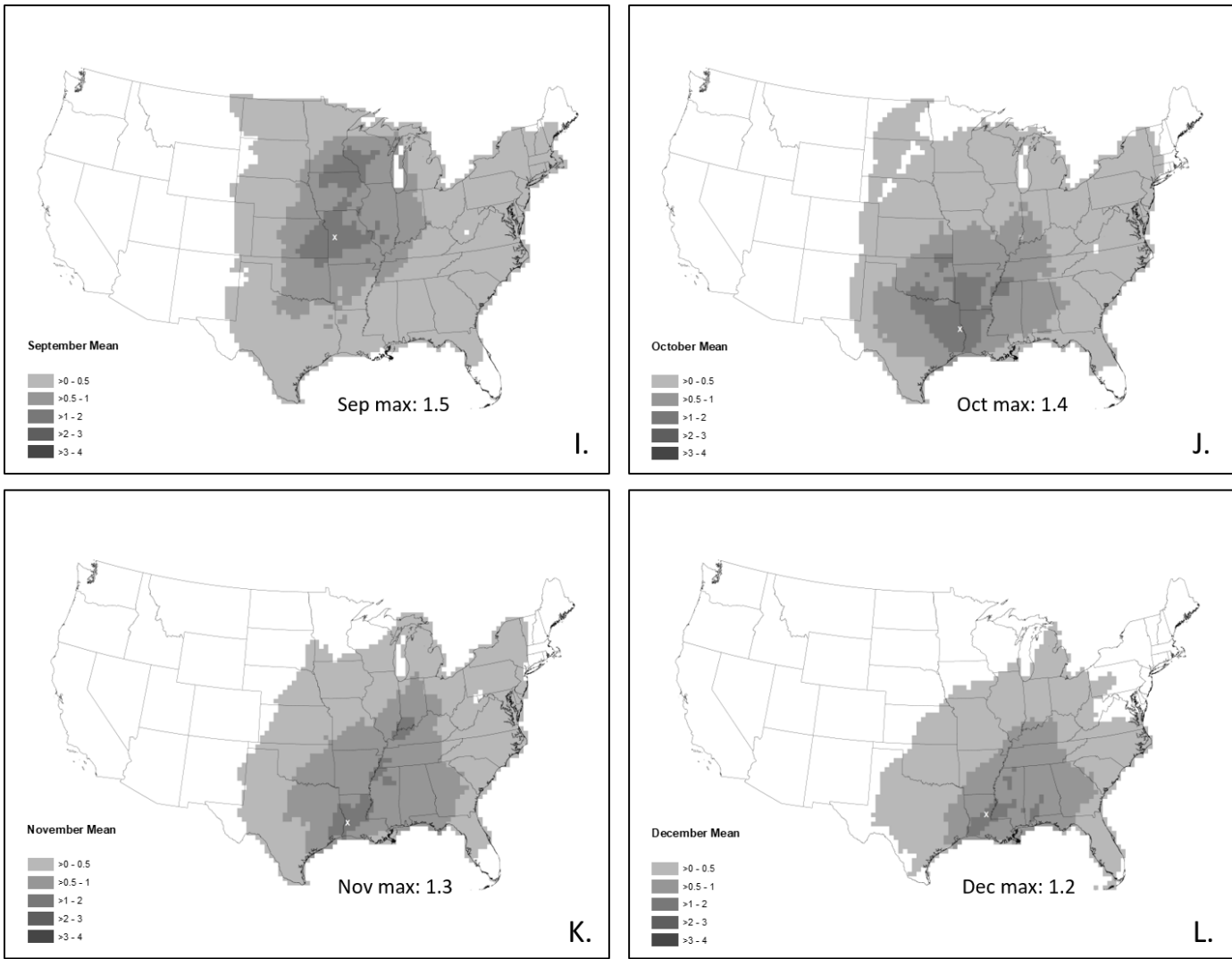


Figure 7.

long-lived, extreme wind events. During the fall transition season, the activity shifts equatorward again (Figure 7 i-j), where it remains through the cool-season months. Ferreira et al. (2013) found that in the fall and winter, upper-level troughs associated with extratropical cyclones retreat equatorward, leading to increased cyclone activity in the southern U.S. Linear forcing due to these cyclones (e.g., cold fronts, dry lines, pre-frontal troughs, etc.), combined with modest lower tropospheric moisture and sufficient CAPE for convection (Gensini and Ashley 2011), promotes a regional maximum in environments supportive of QLCSs in the Southeast CONUS during the cool season. In November and December, QLCS activity is clustered near the Gulf Coast and in the Mid-South, with a climatological maximum in the Southern Mississippi Valley region (Figure 7 k-l).

The spatial distribution of QLCS frequency maxima varies widely across the study period. On an annual basis, absolute grid cell maxima range from a low of around 17 in 2015 to a high of 41 in 2011 (Figure 8). These occurred in very geographically diverse regions, as well, with the 2015 maximum in northern Texas and the 2011 maximum in eastern Kentucky. Although there are vast differences in QLCS frequency during any given year, common corridors of activity are evident. The South is established as one such corridor, as the greatest QLCS activity is found here in 6 of the 22 years (1996, 1997, 2003, 2006, 2008, 2012, 2017). During these years, QLCSs are generally distributed along and north of the Gulf Coast, including Louisiana, Mississippi, Alabama, and Tennessee. Atlantic coastal states are never a focus of activity. QLCSs in these southern states do not tend to produce warm-season derechos, but, during the cool-season, derechos have been shown to frequent the Gulf Coast (Coniglio and Stensrud 2004, Ashley and Mote 2005).

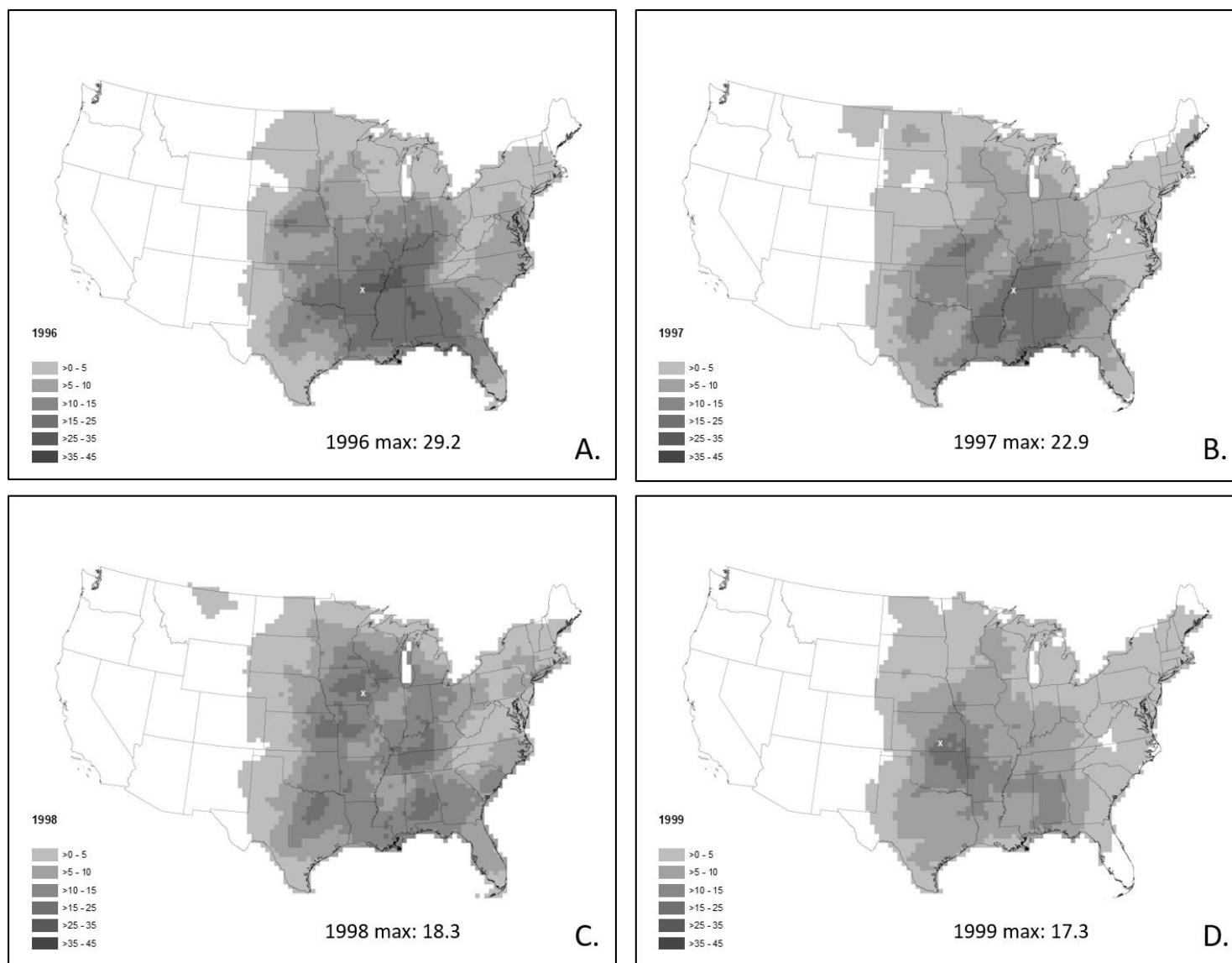


Figure 8. Total QLCS distribution for the years 1996-2017, with the location of the highest annual total marked by a white X.

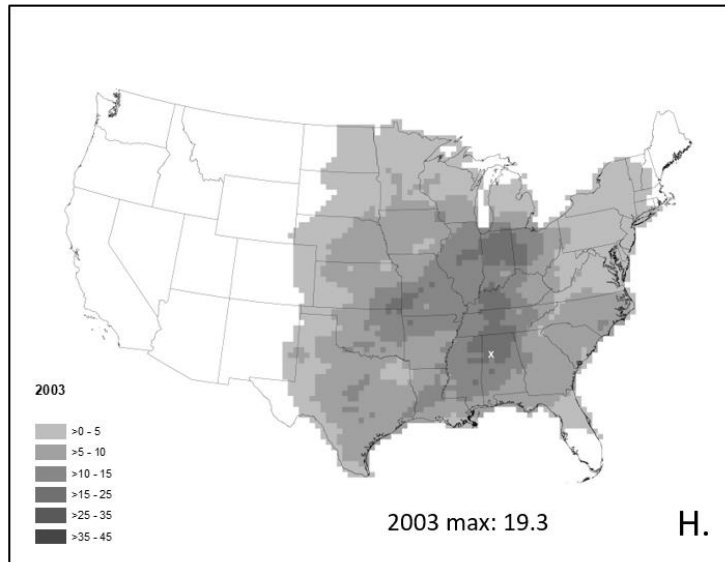
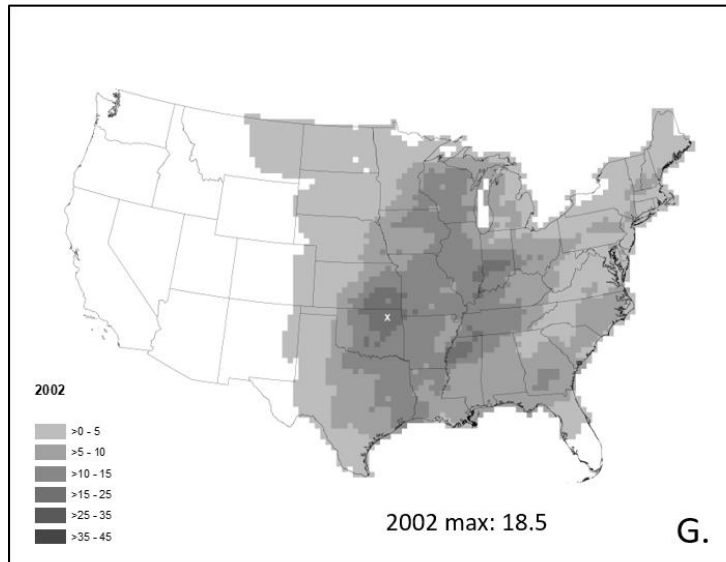
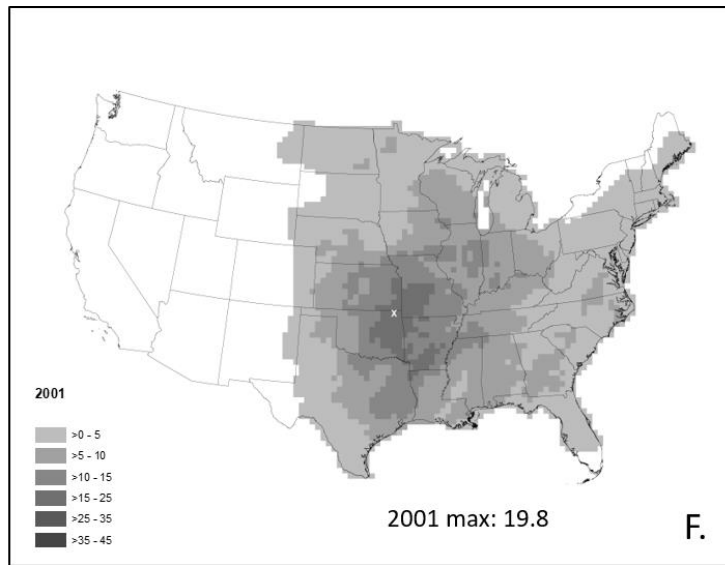
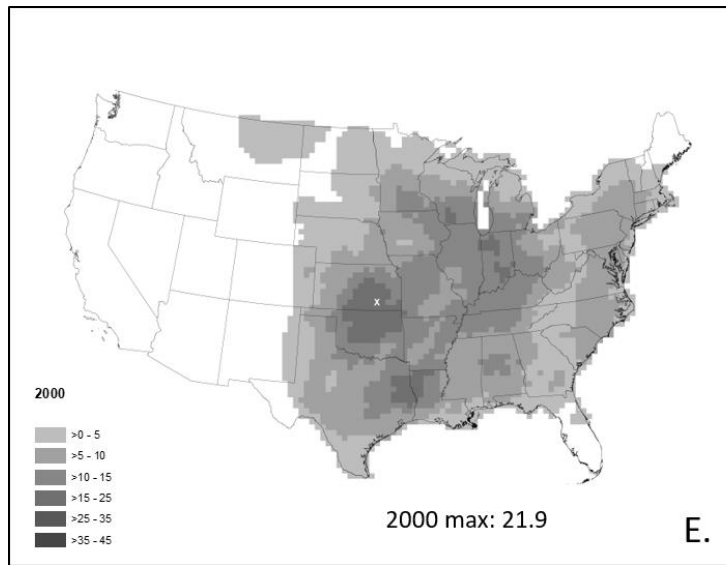


Figure 8. Continued on following page.

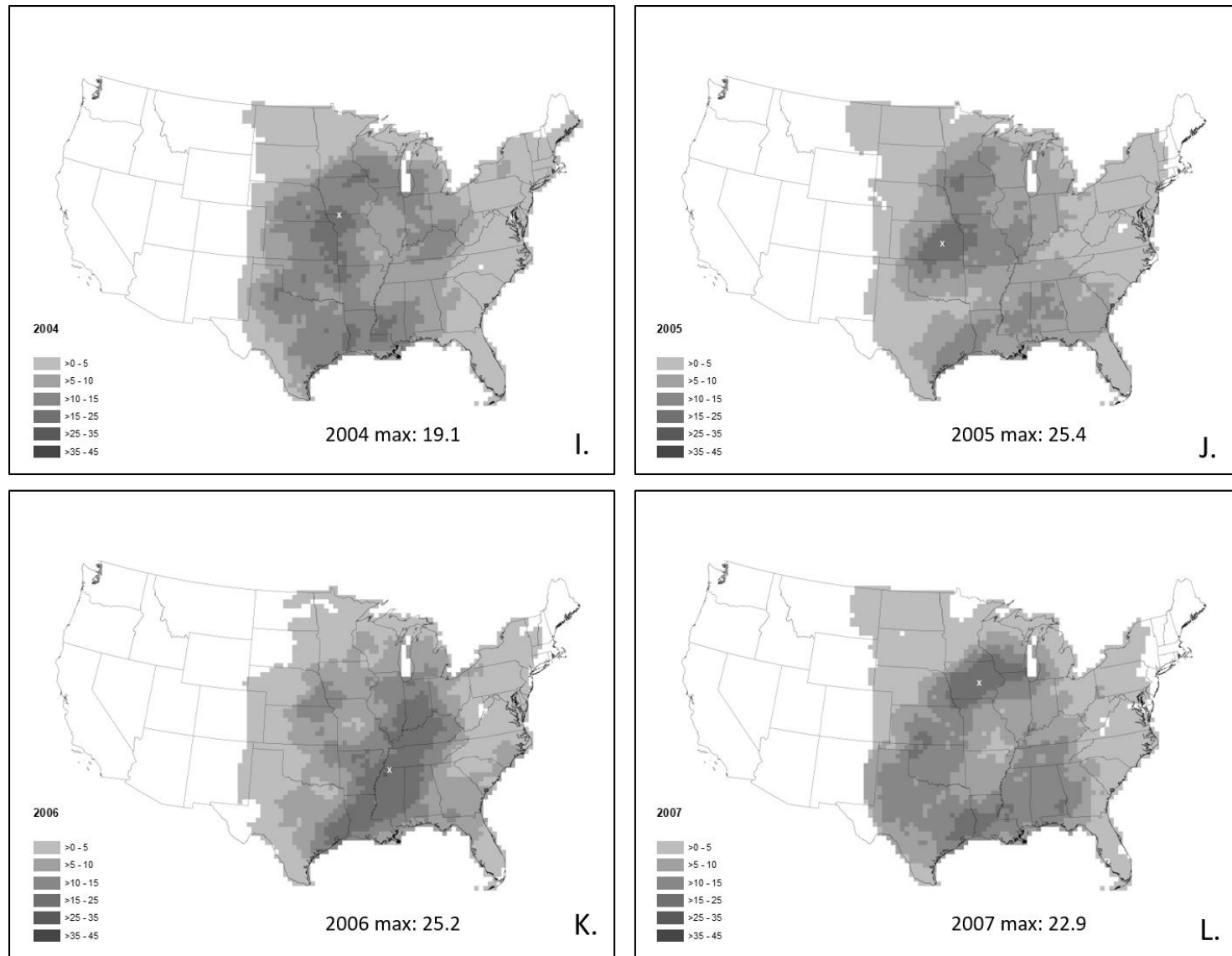


Figure 8. Continued on following page.

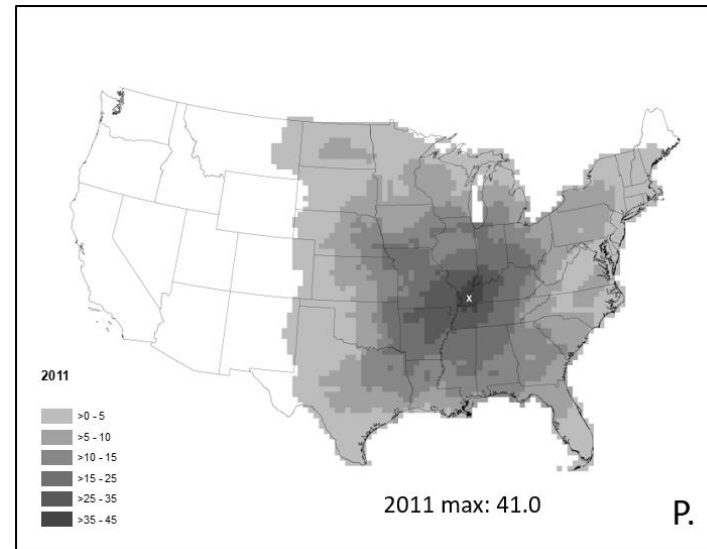
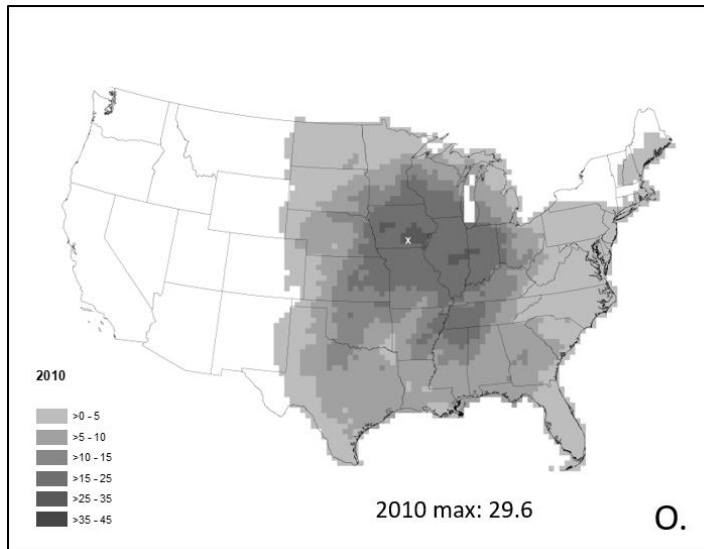
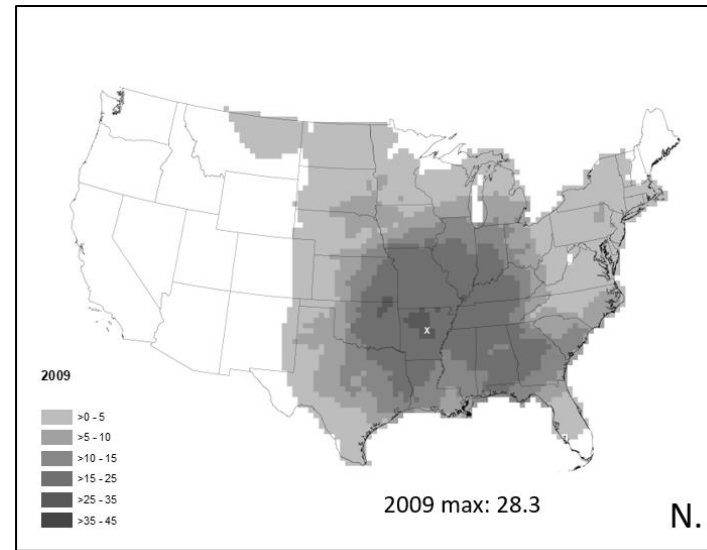
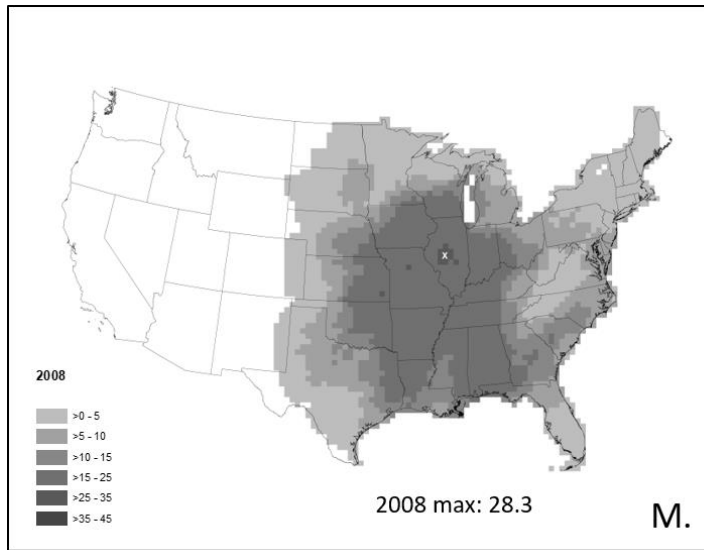


Figure 8. Continued on following page.

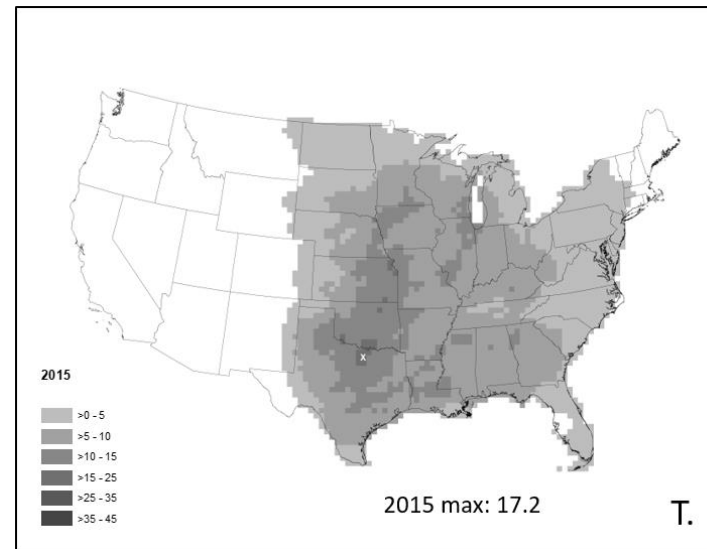
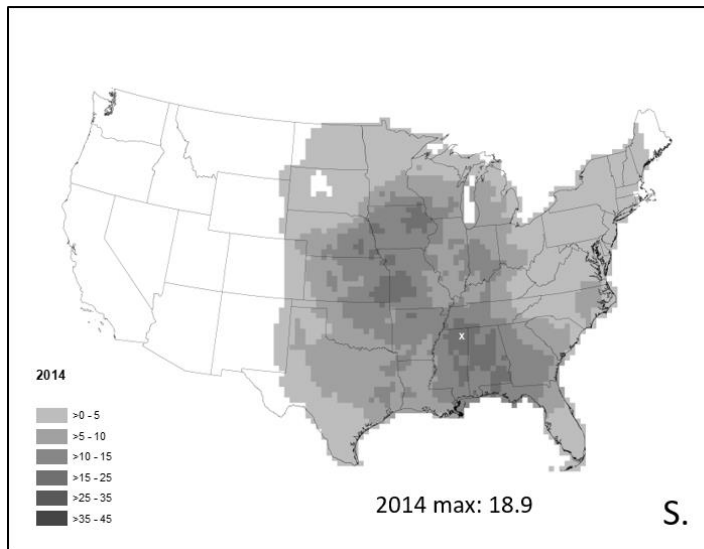
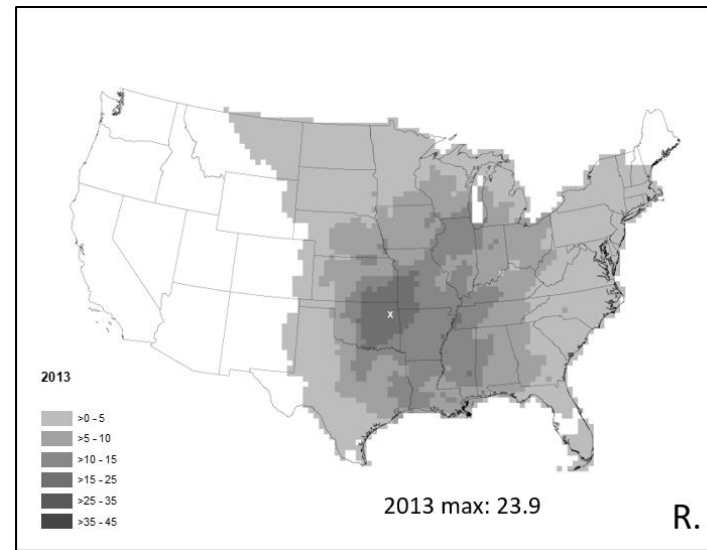
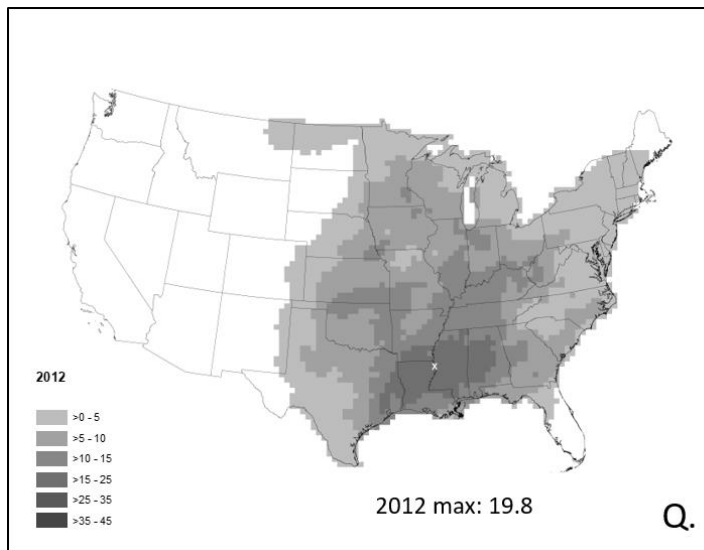


Figure 8. Continued on following page.

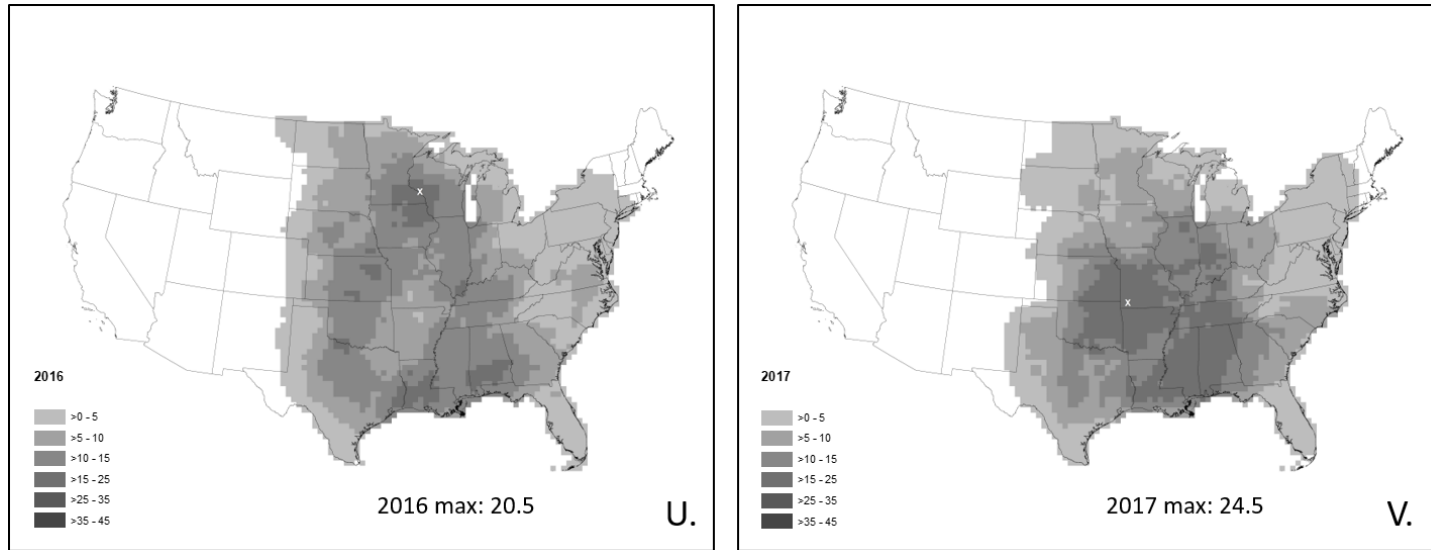


Figure 8.

A second high-frequency corridor is present in the central U.S. states of Kansas, Oklahoma, Missouri, and Arkansas, with maximum grid cell values located here in 10 years of the 22-year study (1999, 2000, 2001, 2002, 2004, 2005, 2008, 2009, 2013, 2017; Figure 8). Once active, this corridor may remain so for several years at a time, such as from 1999 to 2002 when the highest QLCS frequencies in the U.S. were all in one of these four states. When this region takes the lead in QLCS counts, the spatial distribution is usually fairly compact. The greatest values are contained within an area smaller than Oklahoma, with the next highest values spread into the Midwest and the South. Unlike the South, QLCSs here do produce derechos at a rate of one to two per year during the warm season (Coniglio and Stensrud 2004, Ashley and Mote 2005, Guastini and Bosart 2016).

The third high-frequency corridor is in the Midwest, stretching from Iowa and Minnesota southeastward toward to Illinois and Indiana (Figure 8). This region has the largest grid cell values for five years in the 22-year study (2003, 2007, 2008, 2010, 2016). Although QLCSs are not as prevalent here annually as the maxima farther south and east, previous research by Guastini and Bosart (2016) indicates QLCSs in the Midwest tend to be extreme, producing far more warm-season derechos than those in any other corridor, with up to 39 events from 1996 to 2013 in northern Illinois.

Three years (2008, 2009, 2011) stand out as having exceptionally large spatial coverage of QLCS activity, when portions of all the aforementioned corridors were active at a rate of 15-25 QLCSs per year (Figure 8m, n, p). The year 2008 had the most overall QLCSs, and they were widely distributed from the Gulf Coast to southern Wisconsin and from the eastern Plains to the Appalachians. With 41 QLCSs, June 2008 had more events than any month in the period of record. An assessment of the NOAA WPC's Surface Analysis Archive

([https://www.wpc.ncep.noaa.gov/archives/web\\_pages/sfc/sfc\\_archive.php#CONUS](https://www.wpc.ncep.noaa.gov/archives/web_pages/sfc/sfc_archive.php#CONUS)) reveals repeated frontal passages contributed to forcing for an abnormally large number of QLCSs throughout the month. The year 2011 was a remarkable one in terms of density of QLCS occurrence. The central part of the U.S. was active again, with portions of all three high-frequency corridors experiencing 15-25 QLCSs. Although 2011 did not have the most QLCSs overall, that year had the highest spatial concentration, with 41 events passing through western Kentucky. All other years had maximum concentrations of QLCSs less than 30 events. The WPC Surface Analysis Archive reveals an active spring season led to the passage of many cyclones directly over this region. The synoptic pattern appears to have been especially favorable for QLCS development, which also manifested in the 27 April 2011 “Super Outbreak.” Persistent cyclone activity continued through the end of May, contributing to the high frequency of QLCSs in Kentucky in 2011.

Five subregions were defined to examine the regional differences of QLCSs across the eastern two-thirds of the CONUS. These regions include: the North Plains, High Plains, Midwest, South, and Northeast (Figure 9). Each of these regions contains an equal area of 416,000 km<sup>2</sup>, which provides a representative sample to evaluate the regional variation in the QLCS climatology. Three regions had mean QLCS counts above 30 while the other two remained below a mean of 12 QLCS events. On average the South had the most QLCSs per year with 38.8, while the Northeast had the fewest with 8.6 (Table 3).

Diurnal cycles exhibit different characteristics in the five regions assessed (Figure 10). The High Plains experiences the highest hourly peak of any region, with a maximum at 05Z. That region also had the widest range of QLCSs, with a sharp decrease in activity during the morning hours. Although the North Plains followed the same basic diurnal pattern, mean QLCS

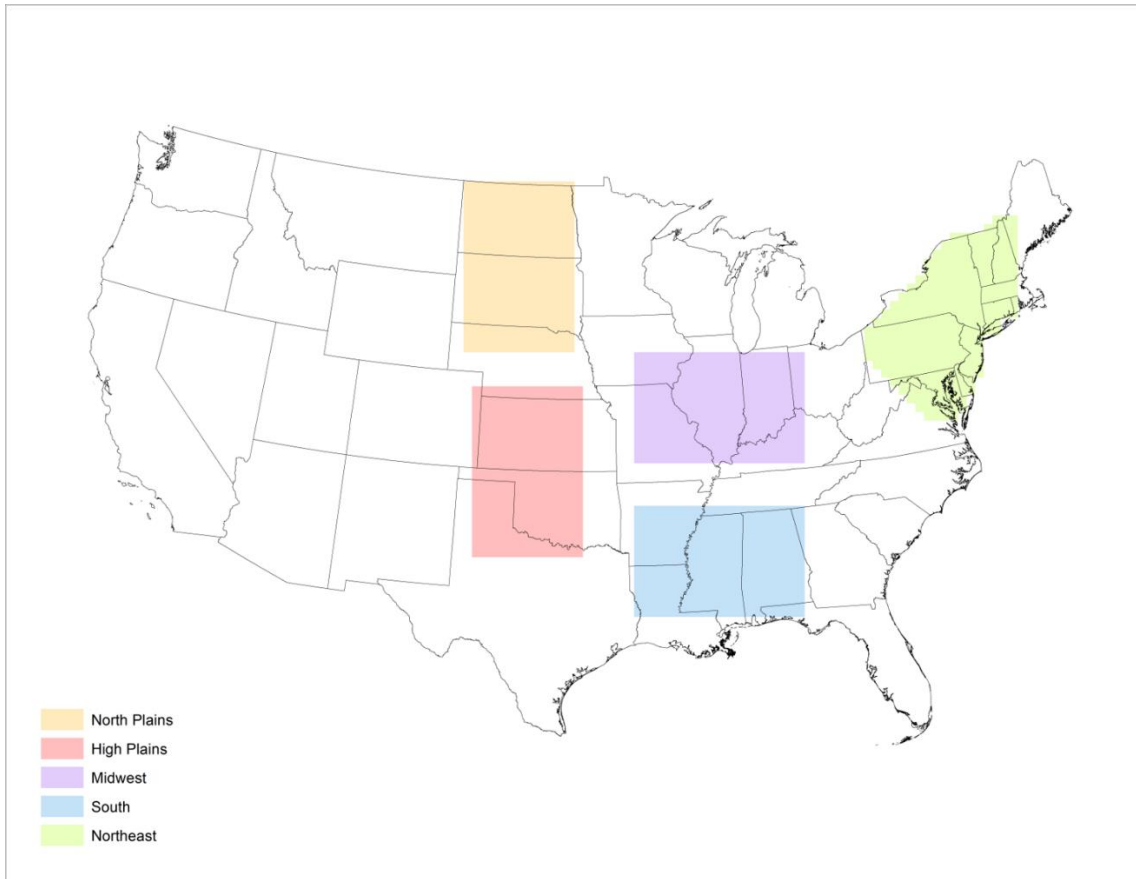


Figure 9. Map depicting five chosen regions: the High Plains, Midwest, North Plains, Northeast, and the South.

Table 3. Counts of QLCS events for each year in each region, along with the total for all regions together. The mean count for all 22 years is included in the final row.

|      | High Plains | Midwest | North Plains | Northeast | South | Total |
|------|-------------|---------|--------------|-----------|-------|-------|
| 1996 | 32          | 36      | 11           | 12        | 52    | 143   |
| 1997 | 28          | 26      | 11           | 6         | 47    | 118   |
| 1998 | 24          | 41      | 14           | 13        | 38    | 130   |
| 1999 | 31          | 20      | 11           | 8         | 34    | 104   |
| 2000 | 36          | 38      | 9            | 18        | 29    | 130   |
| 2001 | 32          | 37      | 12           | 6         | 26    | 113   |
| 2002 | 23          | 33      | 9            | 9         | 30    | 104   |
| 2003 | 26          | 37      | 10           | 6         | 44    | 123   |
| 2004 | 49          | 36      | 10           | 9         | 37    | 141   |
| 2005 | 37          | 31      | 16           | 5         | 24    | 113   |
| 2006 | 22          | 37      | 6            | 6         | 43    | 114   |
| 2007 | 40          | 38      | 11           | 7         | 30    | 126   |
| 2008 | 38          | 57      | 14           | 17        | 54    | 180   |
| 2009 | 36          | 41      | 10           | 11        | 61    | 159   |
| 2010 | 33          | 59      | 22           | 7         | 32    | 153   |
| 2011 | 23          | 59      | 19           | 14        | 48    | 163   |
| 2012 | 26          | 32      | 4            | 6         | 42    | 110   |
| 2013 | 37          | 35      | 10           | 7         | 27    | 116   |
| 2014 | 31          | 29      | 9            | 7         | 34    | 110   |
| 2015 | 34          | 24      | 12           | 6         | 34    | 110   |
| 2016 | 38          | 39      | 23           | 5         | 39    | 144   |
| 2017 | 36          | 38      | 8            | 3         | 49    | 134   |
| Mean | 32.4        | 37.4    | 11.9         | 8.5       | 38.8  | 129.0 |

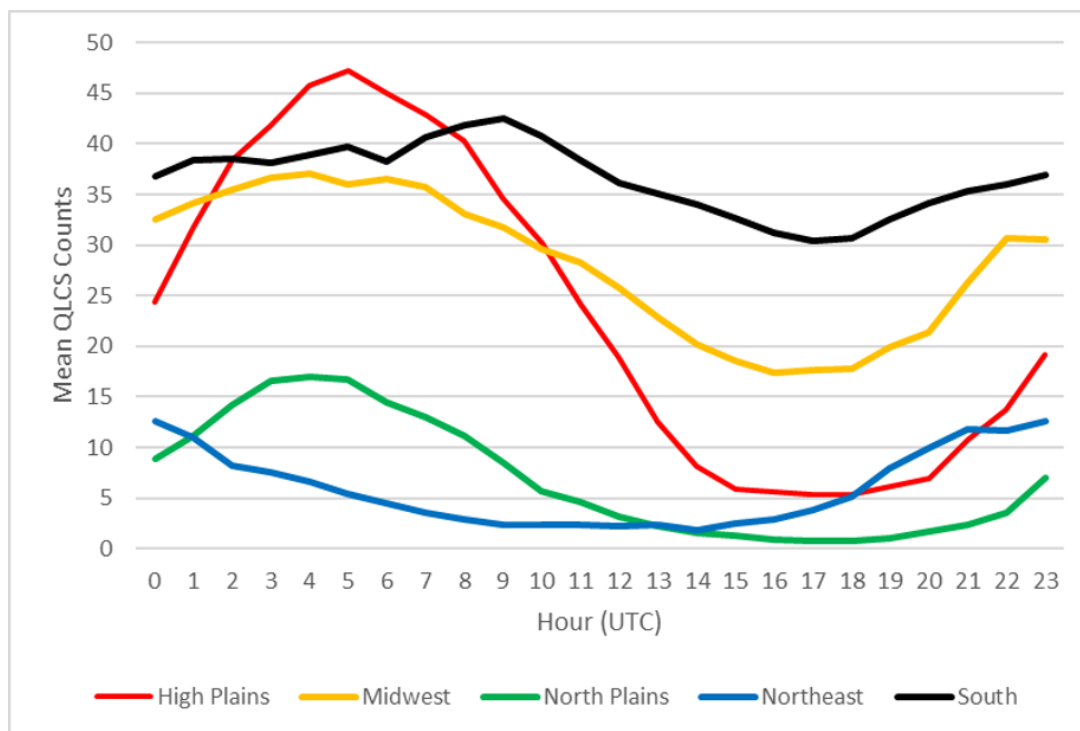


Figure 10. Mean QLCS counts per hour for five regions: the High Plains, Midwest, North Plains, Northeast, and the South.

counts were much lower (Figure 10). The regional difference in these nighttime and early morning QLCS frequencies may be due to the greater strength and more frequent presence of the low-level jet (LLJ) in the High Plains in comparison to the North Plains (Arritt et al. 1997, Pu and Dickinson 2014). The LLJ is common in the High Plains region during the spring and summer and is highly connected to the development of MCSs and their maintenance overnight (Pitchford and London 1962, Arritt et al. 1997, Pu and Dickinson 2014, Geerts et al. 2017). The LLJ functions as a source of moisture and conditionally unstable air but has also been found to contribute to lower tropospheric convergence (at its terminus) and frontogenesis (Maddox 1983, Cotton et al. 1989, Trier et al. 2006). These elements contribute to fueling MCSs and QLCSs through the overnight hours in the Great Plains and the Midwest.

Compared to the Plains regions, the Midwest has greater activity in the mid-morning to late afternoon hours. In the Midwest, mean QLCS counts per hour are greater than in the High Plains during the late morning and afternoon (Figure 10). This pattern may be result of the low LLJ influencing both the High Plains and Midwest. Warm-season MCSs in these regions are commonly found at the terminus of the LLJ along a quasi-stationary, baroclinic boundary (Tuttle and Davis 2006, Geerts et al. 2017). Although it is most often associated with the Plains, the LLJ is climatologically found along an axis that runs from the border of Mexico and Texas north into the upper Midwest. A corresponding poleward shift in nighttime precipitation occurs during LLJ events from the Gulf Coast into the Midwest as the warm season approaches (Higgins et al. 1997). The positioning and strength of the LLJ may allow some nocturnal QLCSs in the High Plains to survive overnight and add to Midwest QLCS counts after 10Z.

As with the three aforementioned regions, the South also has a peak in activity during the morning and reduced activity in the afternoon. This pattern manifests differently in this region, as the maximum QLCS counts in the South are observed at 09Z, which lags behind all other regions by several hours. Additionally, counter to other regions, the South maintains high levels of QLCS activity throughout the entire day. While High Plains QLCSs may thrive on the LLJ, southern QLCSs could be fueled by increased heat and moisture from the Gulf of Mexico, as found by previous studies of Southeast MCSs (Lericos et al. 2002, Parker and Ahijevych 2007). This ever-present energy source could explain why QLCSs in the South remain fairly consistent throughout the day compared to all other regions. Convection is generally produced by extratropical cyclones during the winter months, when QLCS activity is highest in the southern U.S., and so the forcing that supports these storms is not tied to diurnal processes (Parker and Ahijevych 2007). The diurnal pattern identified here differs from that of Geerts (1998), which

found maximum MCS activity in the Southeast U.S. between 21 and 23Z. However, comparison between Geerts and the results herein is challenging since the Geerts study included assessments of much smaller convective clusters that would not fit the MCS or QLCS definition employed herein. In addition, the Geerts study was for a very limited period, including only 1994 and 1995.

The Northeast is the only region that exhibits a different diurnal pattern than the others. The daily maximum of QLCSs occurs between 23-00Z, before activity slowly decreases between 17-18Z. This is consistent with the results of Lombardo and Colle (2010), who found that the majority of Northeast linear systems form between 18-00Z. The timing of QLCS formation is sometimes tied to the development of surface troughs over the area of convection. These surface troughs organize ahead of cold fronts either from adiabatic downslope warming in the lee of the Appalachians, synoptic-scale ascent as the trough moves ahead of the cold front, or forward-tilting fronts with warm air ahead of them (Schultz and Steenburgh 1999, Schultz 2005, Lombardo and Colle 2010).

#### *b. QLCS Storm Report Climatology*

This section explores the spatiotemporal distribution of QLCS hazards across the eastern two-thirds of the CONUS. In total, there were 95,957 QLCS-attributed storm reports between 1996 and 2017, with 68,633 due to nontornadic severe wind (71.5%), 21,660 severe hail (22.6%), and 5,664 reported tornadoes (5.9%). On an annual basis, total QLCS storm reports varied widely, from 2,961 in 1997 to 7,690 in 2011. Three years (2008, 2011, and 2017) stand out as having unusually high numbers of storm reports attributable to QLCSs (Figure 11a), which were influenced by individual months that had exceptional storm activity. For instance,

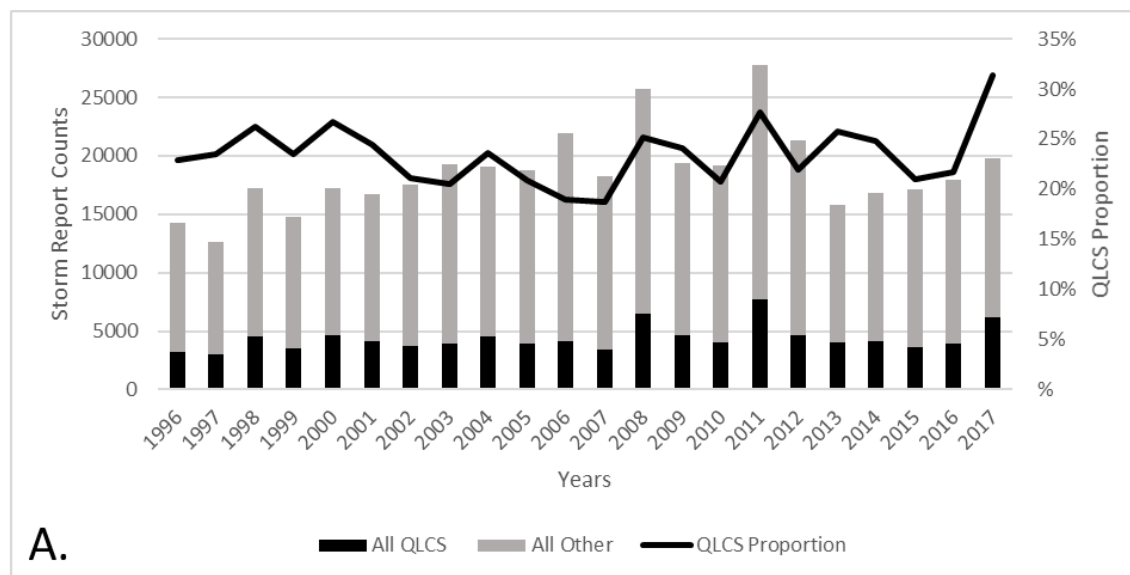


Figure 11. Graphs of all hazards (wind, hail, tornado) for QLCS and non-QLCS storms. A: Annual counts (left axis) of QLCS hazards (black bar) and non-QLCS hazards (gray bar), with the QLCS proportion of total reports (black line) on the right axis. B: Monthly counts (left axis) of QLCS hazards (black bar) and non-QLCS hazards (gray bar), with the QLCS proportion of total reports (black line) on the right axis. C: Mean hourly counts (left axis) of QLCS hazards (black bar) and non-QLCS hazards (gray bar), with the QLCS proportion of total reports (black line) on the right axis. D: Map of occurrence of all hazards (wind, hail, tornado) for QLCS storms during the entire 22-year study period. E: Map of the QLCS proportion of all hazards (wind, hail, tornado) during the entire 22-year study period. Continued on following page.

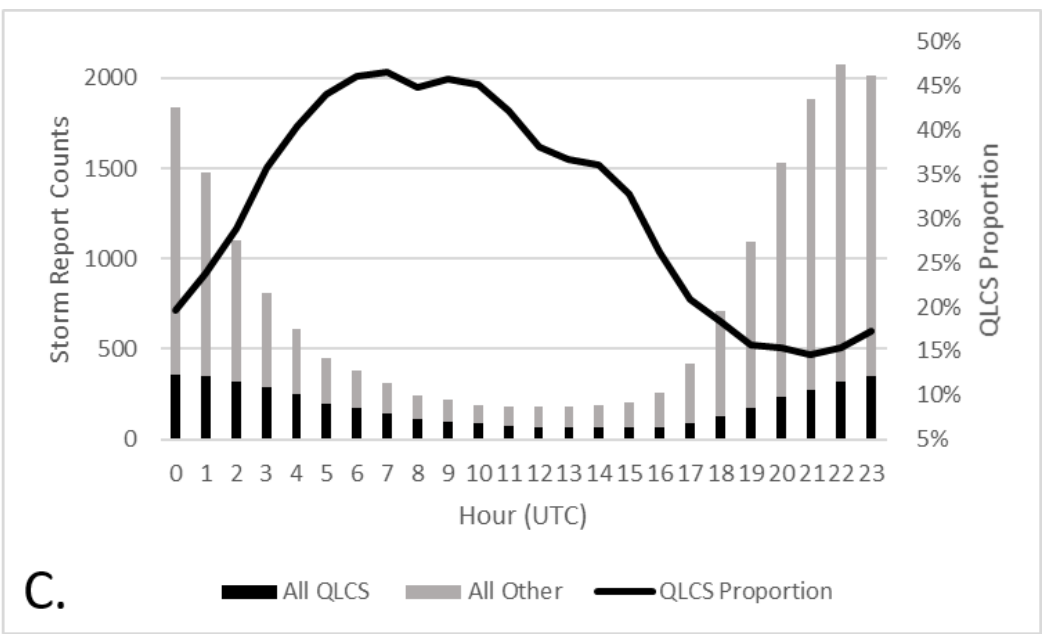
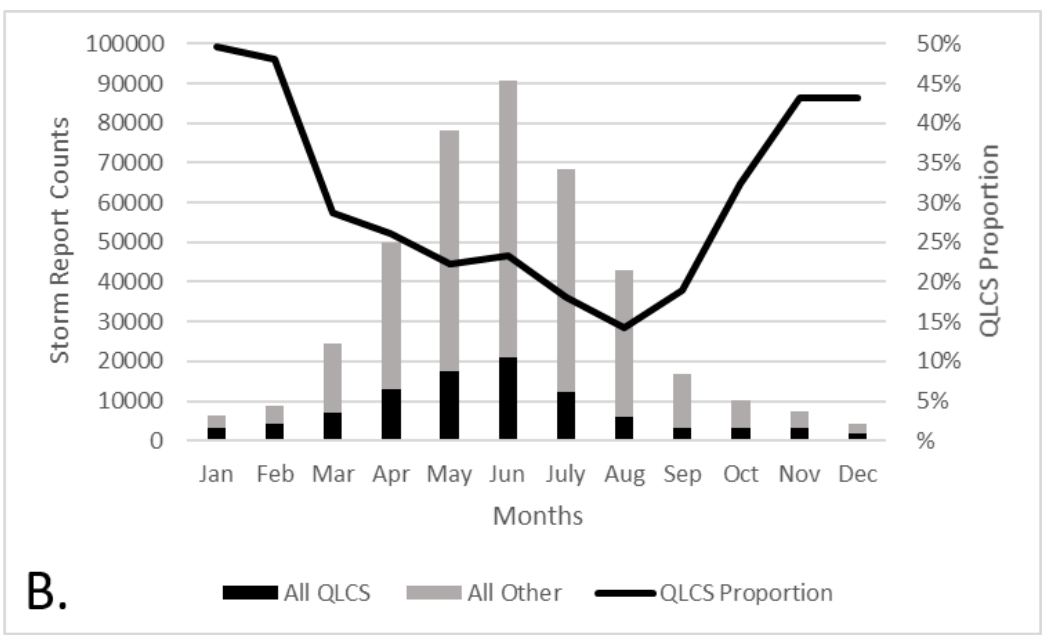


Figure 11. Continued on following page.

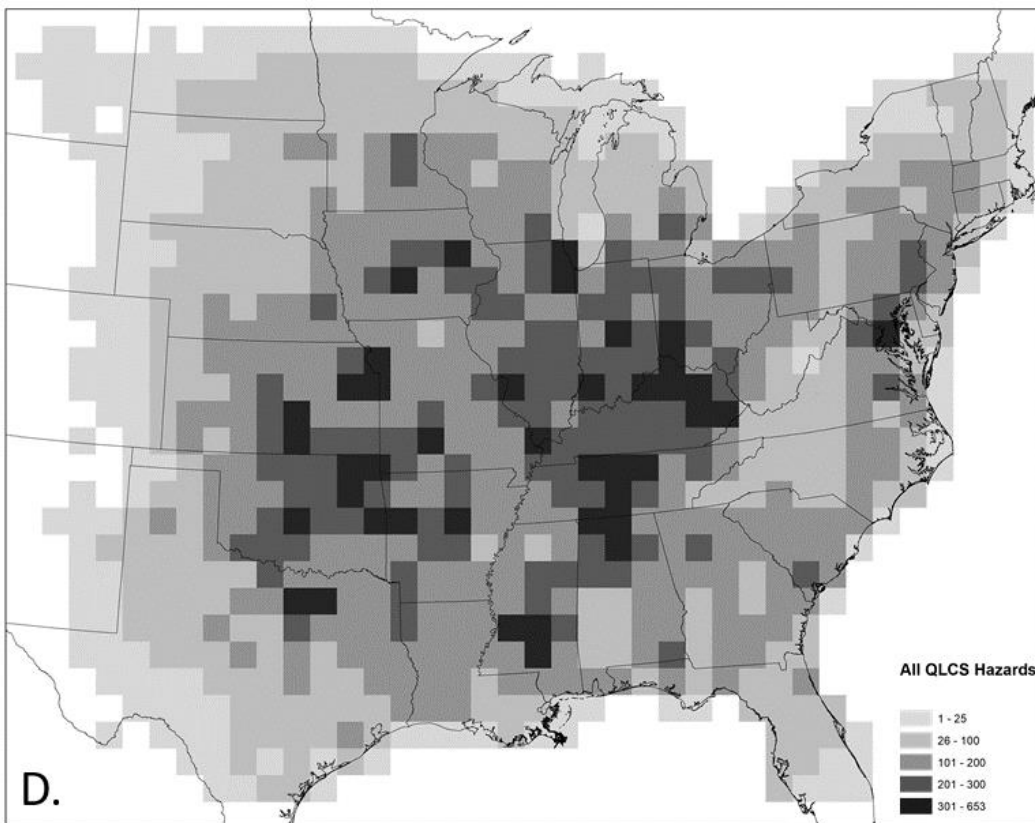


Figure 11. Continued on following page.

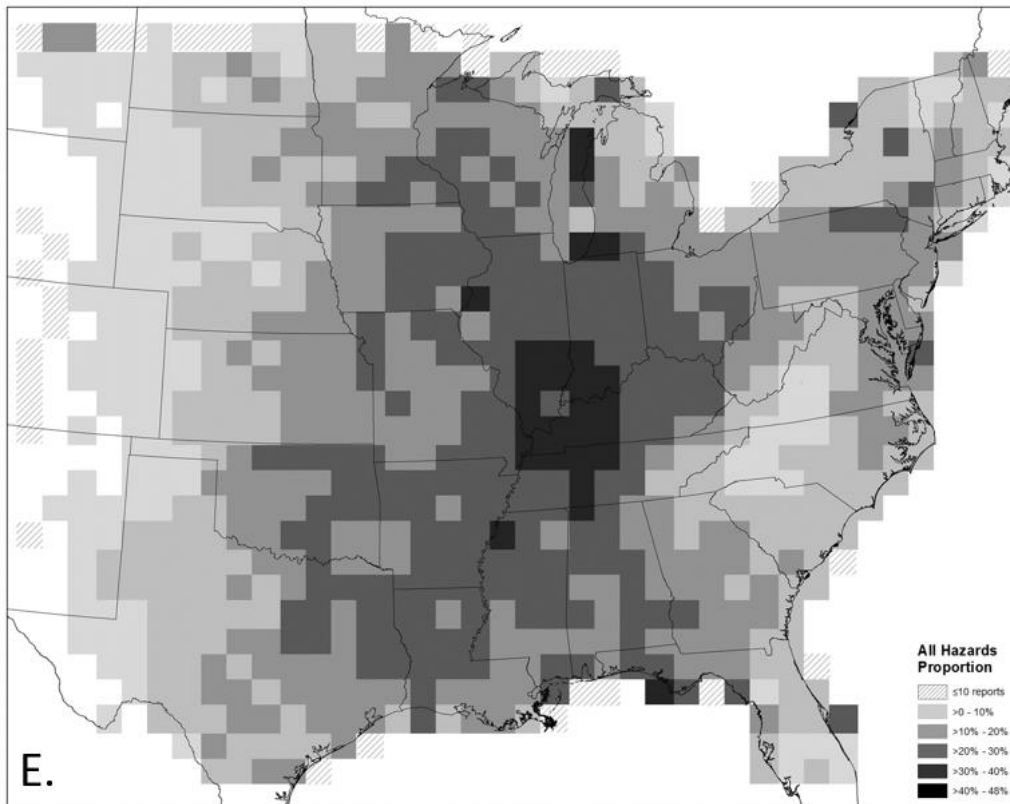


Figure 11.

June 2008 was exceptionally active, with every day, except the 30<sup>th</sup>, receiving over 100 storm reports. In particular, the 27 April 2011 had a series of significant convective events that culminated with the supercell tornado outbreak in the evening; however, the two severe storm events during the overnight and morning hours were due to high-end QLCS events that produced numerous tornadoes and significant wind reports. March 2017 was particularly active, with three separate days with over 700 storm reports each (<https://www.spc.noaa.gov/climo/online/>). These monthly cases reveal how a relatively short, but active period can influence annual totals of storm reports. QLCS-affiliated storm reports contribute from 19% to 31% of total storm reports in any given year, with a mean of 23.4% annually (Figure 11a). There are no studies to which

these numbers may be directly compared, but Smith et al. (2012) found QLCSs were responsible for 19% of *significant* severe reports identified in their 9-year study.

On a monthly timescale, QLCS-attributed storm reports follow the distribution of their parent storms. Storm reports increase every month during the year until June, with a notable 46% increase from March to April. QLCS storm reports reach a peak in June and, thereafter, drop to minima during the cool season. QLCS reports make up the lowest proportion of total reports in August, when they only account for 14% of all storm reports. In contrast, QLCS storm reports make up 50% of all reports in January, when QLCSs themselves are at a seasonal minimum (Figure 11b).

As this paper has demonstrated, QLCSs are not tied to diurnal processes as strongly as other storm modes. Even as QLCS numbers decline throughout the early morning hours, their proportion of total storm reports rises from a low of 15% at 21Z to a high of 46% at 06Z. This peak is maintained for six hours between 5Z and 10Z before dropping off, which suggests that QLCSs can have damaging impacts for extended durations (Figure 11c).

QLCS hazards are most common across the central and eastern U.S., amounting to between 100 and 250 reports per 80 x 80 km grid cell over the duration of the 22-year study period. On average, this is 4.5 to 11.4 QLCSs per year in areas of the Great Plains, Midwest, Southeast, and Mid-Atlantic. QLCS hazards are experienced most frequently in two main areas of the U.S.: a region including Kansas, Oklahoma, Missouri, and Arkansas and the east-central U.S., stretching from the Midwest to the Mid-South. This spatial pattern closely mirrors the distribution of annual QLCS occurrence, suggesting that the rate of QLCS hazard production is related to the number of QLCSs observed (Figure 11d).

Southern Indiana has the highest proportion of QLCS hazards, with over 47% of storm reports resulting from QLCSs. A regional maximum exists south and west of there, where portions of Illinois, Kentucky, and Tennessee have more than 40% of hazards attributable to QLCSs. Large areas of states in the South and Midwest have between 30% and 40% of all hazards produced by QLCSs while the East Coast and Great Plains may attribute 10% to 30% of hazards to this storm mode (Figure 11e).

*i. QLCS-attributable tornadoes*

From 1996 to 2017, 22.7% of tornadoes were produced by QLCSs. There were 166 to 552 QLCS-attributable tornadoes per year; however only three years—2008, 2011, and 2017—had more than 300 QLCS tornadoes. A slight upward trend in QLCS tornado counts is observed, with an increase of 7.2 tornadoes per year (Figure 12a). This trend is influenced by the high numbers of QLCS tornadoes during the latter half of the study period in 2008, 2011, and 2017. The proportion of tornadoes due to QLCS shows an upward trend as well, but one which may be explained by non-meteorological factors (Figure 12a). This pattern may be due to an observed increase in tornadoes, especially those of EF-0 magnitude, over recent decades. Tornado reports nearly doubled between the 1950s and early 2000s because of increases in population, greater radar coverage, and a greater focus on tornado reporting (Brooks et al. 2003, Brooks et al. 2014, Ashley and Strader 2016). Since QLCSs tend to produce weak tornadoes (Trapp et al. 2005), the increased reporting of such tornadoes creates an artificial, likely secular-driven, trend in the data. The proportion of tornadoes due to QLCSs averages 22.7% over the study period, which is higher than the 18% found by Trapp et al. (2005) in their 3-year study and much higher than the 13.8% found by Smith et al. (2012) in their 9-year study.

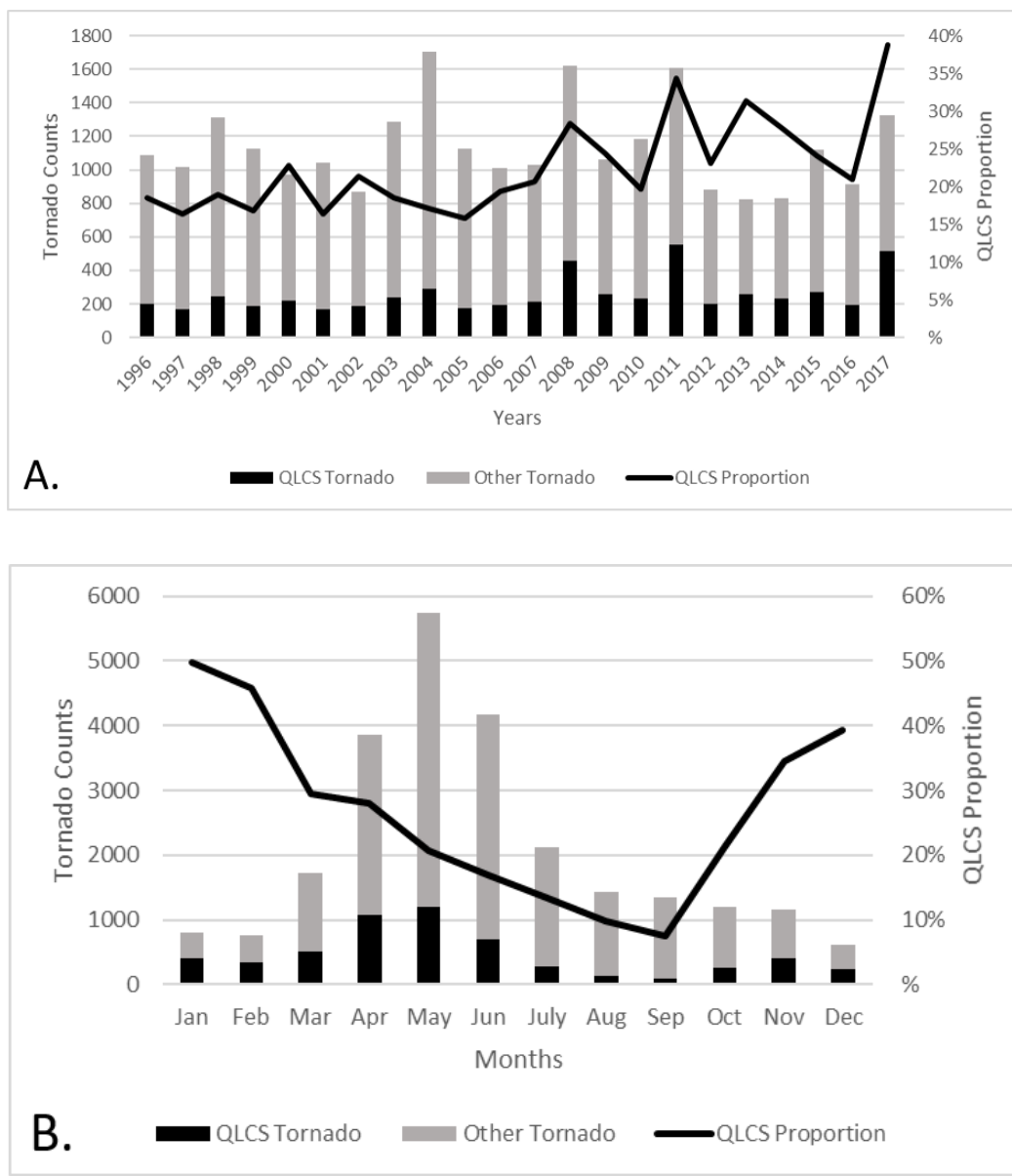


Figure 12. As in Figure 11, but for tornado reports. Continued on following page.

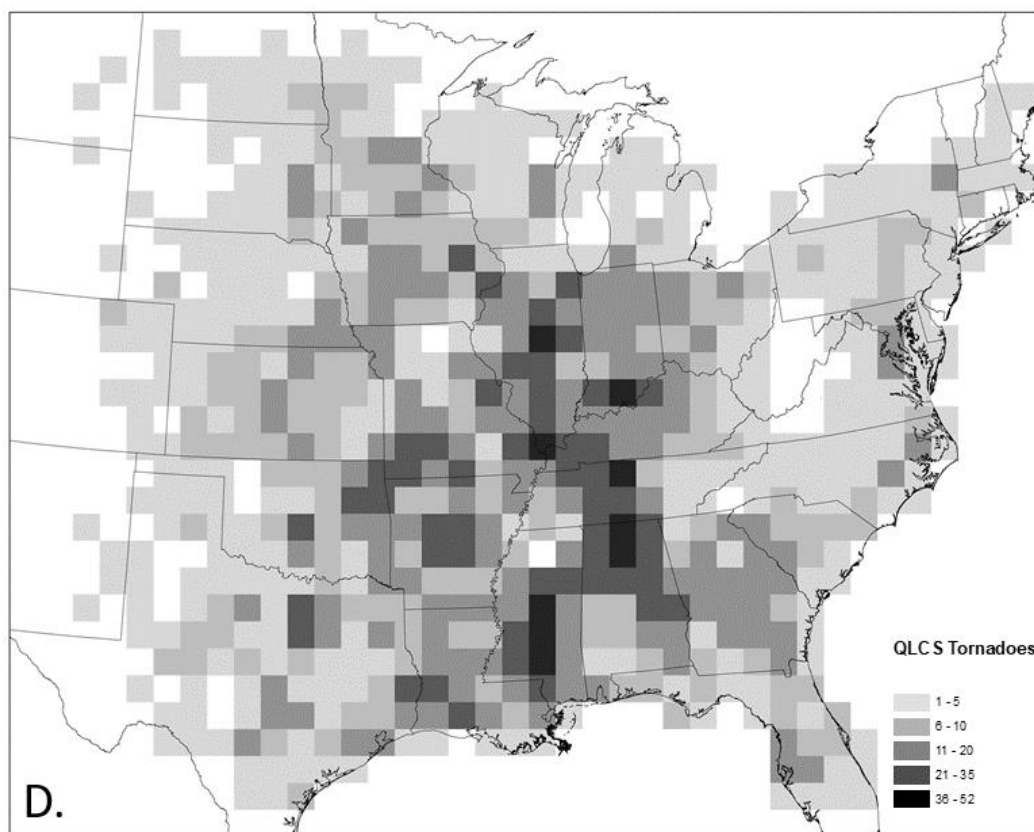
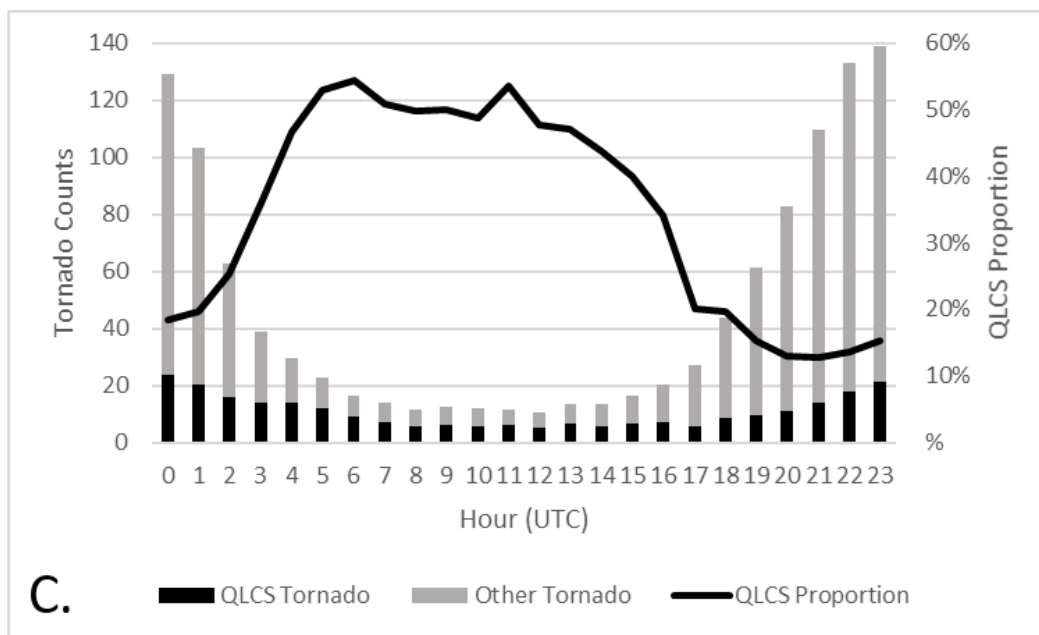


Figure 12. Continued on following page.

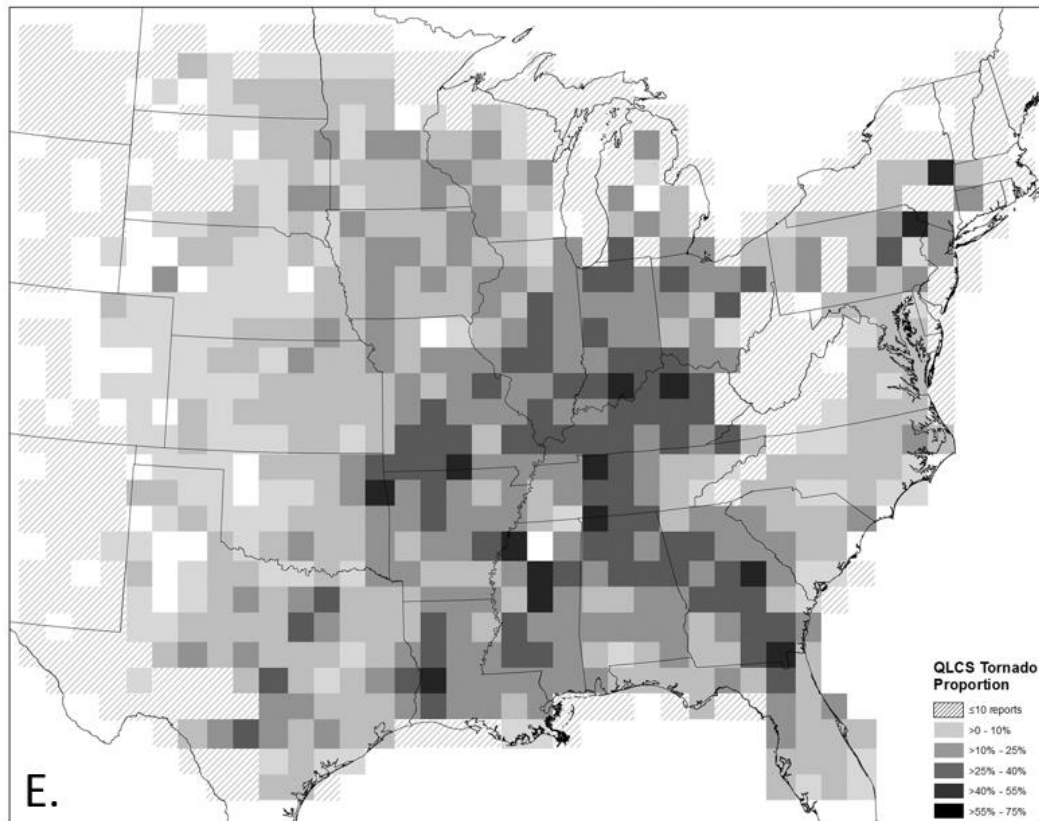


Figure 12.

Monthly trends for QLCS-affiliated tornadoes are slightly different than those for severe wind and hail, as QLCS tornadoes are more frequent in April and May than in June. QLCS tornado counts then decrease until October, with November observing the most QLCS tornadoes in the second half of the year. This result is consistent with Trapp et al. (2005), who found a slight increase in F0 and F1 tornadoes from lines of storms during November. Although the overall number of QLCSs is quite low in November compared to other transition and cool-season months, increased tornado activity at this time may be associated with an equatorward shift in extratropical cyclone tracks towards areas of higher baroclinity (Eichler and Higgins 2006).

Monthly, the proportion of tornadoes that are due to QLCSs is lowest in September, at 8%, but increases to nearly 50% in January (Figure 12b). The September minimum could be caused by both a lack of baroclinity resulting in reduced vertical wind shear that is required for organized thunderstorms (Parker and Ahijevych 2007).

QLCS-affiliated tornadoes are generally afternoon and nocturnal phenomena.

Conversely, QLCS tornadoes comprise the greatest proportion of tornadoes during the early and mid-morning hours, peaking at 5Z and 11Z. Although the proportion due to QLCSs decreases slightly between 5Z and 11Z, QLCSs are responsible for nearly 50% of tornadoes or more during these seven hours of the day (Figure 12c). This nocturnal peak is a notable concern for societal impacts and warning efficacy, as 40% of tornado fatalities are due to events occurring in the overnight hours (Ashley 2007, Kis and Straka 2010).

QLCS tornadoes display a spatial pattern that differs from other severe storm hazards (Figure 12d). One climatological maximum exists in the South, between Mississippi and northern Alabama, with a second maximum in central Illinois. The maximum annual average of 2.7 QLCS tornadoes per 80 x 80 km grid cell is found on the border of Tennessee and Alabama. The southern maximum closely matches the distribution of nocturnal killer tornado events found by Ashley et al. (2008) and killer tornado events from linear storms presented by Schoen and Ashley (2011), suggesting that QLCSs may be to blame for overnight deaths in this region.

The highest proportions of tornadoes due to QLCSs are found in the east-central U.S., extending from Kentucky southward into Alabama and Georgia (Figure 12e). Southwestern Missouri and northern portions of Mississippi also experience high proportions of tornadoes from QLCSs. This geographical distribution has some resemblance to the results of Trapp et al. (2005), but they analyzed tornado days instead of the percentage of QLCS tornadoes. While

Trapp found that the highest percent of tornado days are in Indiana, this analysis found that the greatest proportion of QLCS tornadoes occur in Kentucky. Kentucky, Tennessee, and Missouri have a greater risk from QLCS tornadoes than previously uncovered; areas of these states have over 40% of their tornadoes due to QLCSs.

ii. *QLCS-attributable wind*

When examining changes in QLCS-attributable severe wind reports as a percentage of total wind reports over time, there is no trend. This suggests that, although QLCS wind reports may be increasing slightly over time, total storm reports are increasing at a comparable rate. In any given year, QLCSs are responsible for 26% to 41% of the total severe wind reports, with an average of 33.8% (Figure 13a). The ability for these events to produce substantial proportions of reported severe wind reports is due to their large size compared to other storm modes, such as supercells (Duda and Gallus 2010).

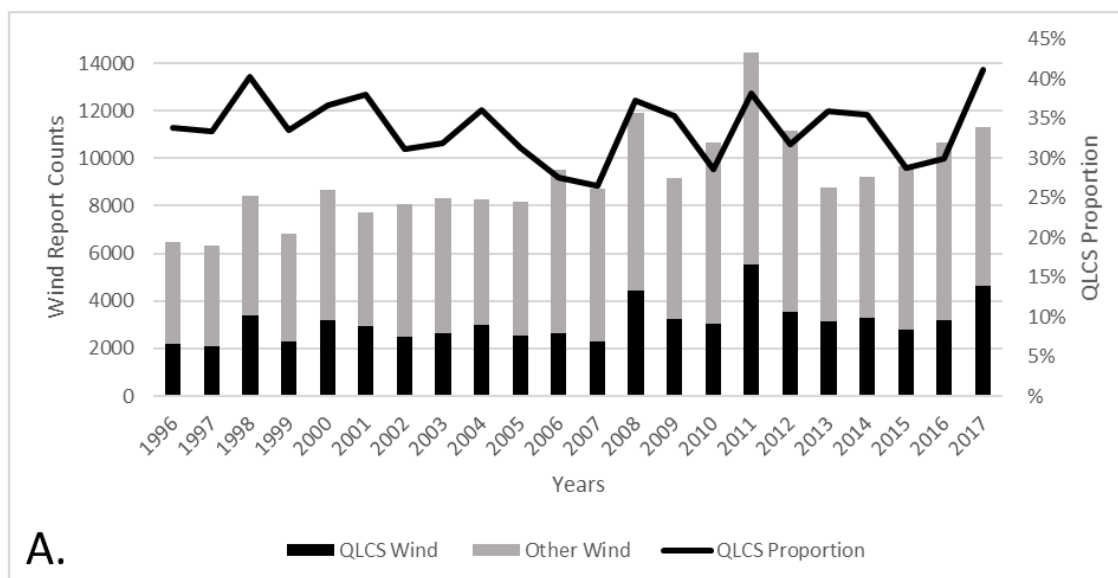


Figure 13. As in Figure 12, but for severe wind reports. Continued on following page.

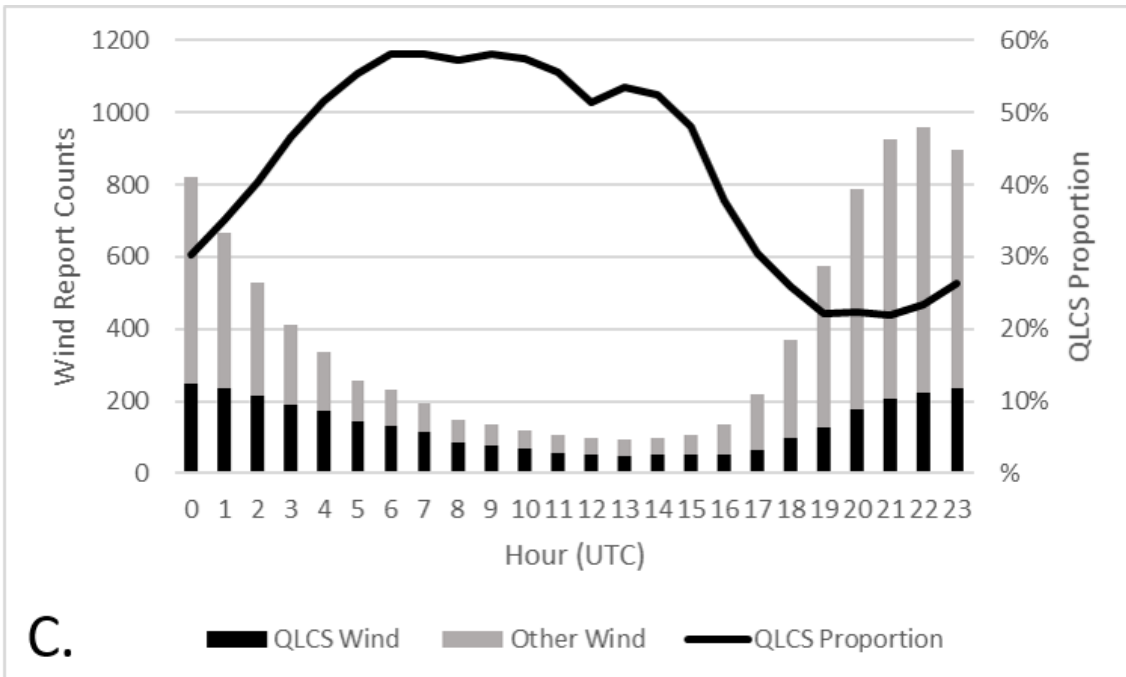
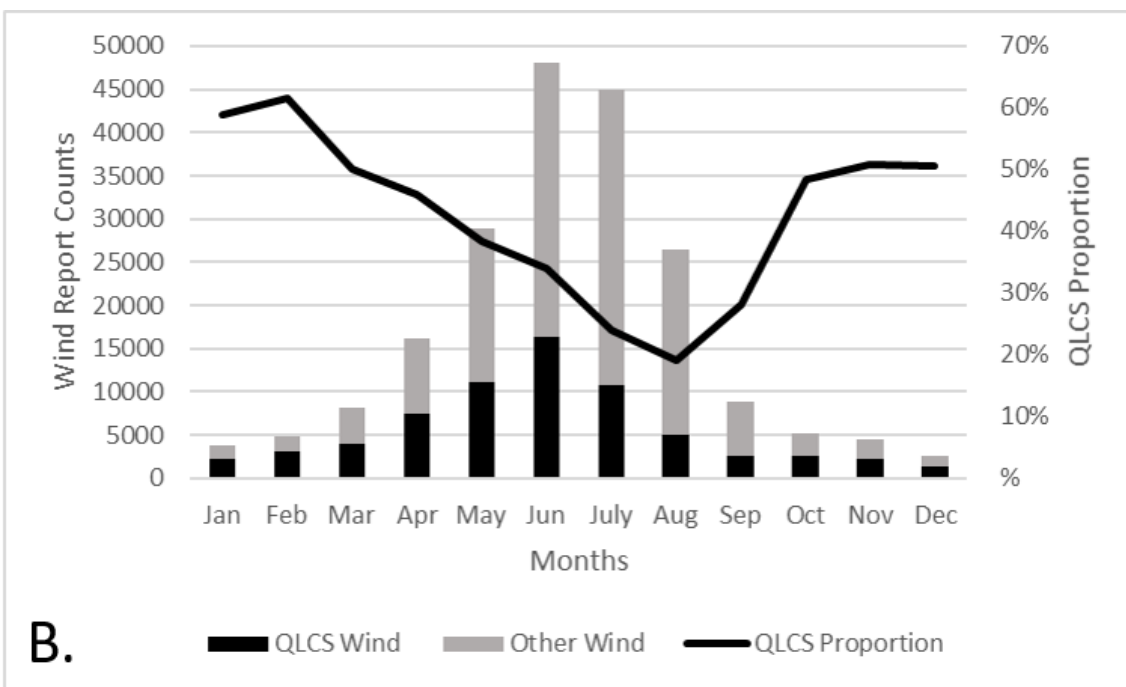


Figure 13. Continued on following page.

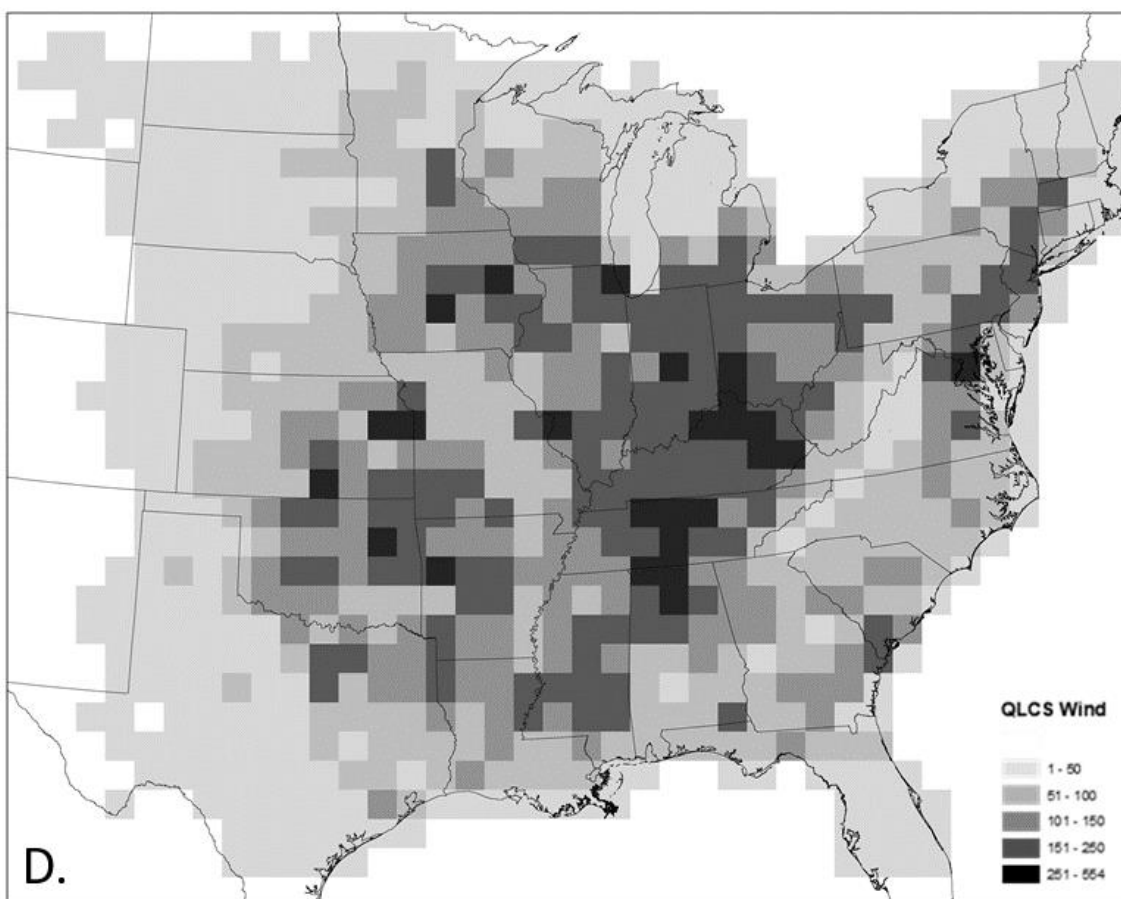


Figure 13. Continued on following page.

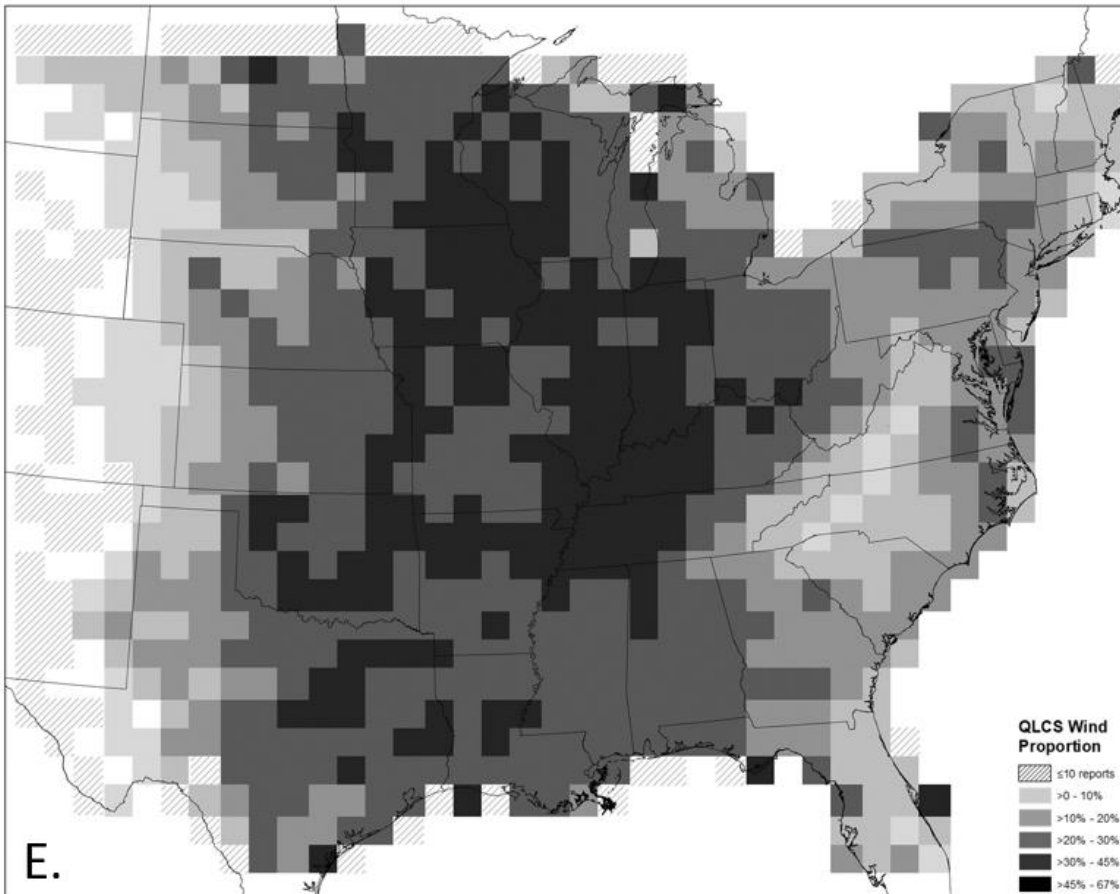


Figure 13.

On a monthly basis, the number of QLCS-affiliated severe wind reports peaks in June and reaches a minimum in December. These reports range widely as a proportion of the total, from 19% in August to 62% in February. For five months of the year—from November to March—QLCS wind reports make up at least half of all wind reports (Figure 13b). Because QLCSs are most prevalent in the overnight and early morning hours, their severe wind reports follow the same temporal distribution. The daily maximum occurs at 0Z and decreases until 13Z before rising again. QLCS severe wind reports represent a higher proportion of total reports

throughout the night and into the morning hours, increasing from 22% at 19Z to 58% between 6Z and 9Z. Proportionally, QLCS wind reports account for most of all wind reports for nearly half the day, from 4Z to 14Z (Figure 13c). QLCS wind reports also follow the same spatial patterns as all hazards combined, clustering in the same regions. While Smith et al. (2012) found a maximum in their filtered QLCS significant wind reports centered in northern Illinois during the summer, such a maximum is not evident when examining all QLCS wind reports herein. QLCS severe wind frequency maxima are observed in the Kansas, Oklahoma, Missouri, Arkansas region, but with less frequent occurrence than in eastern Kentucky and southern Ohio. The Midwest and parts of the South commonly see between 4.5 and 9 wind reports per 80 by 80 km grid cell per year (Figure 13d).

The area of southern Illinois, western Kentucky, and northwestern Tennessee experience up to 60% of their wind reports from QLCSs. A second smaller maximum lies in Iowa, Wisconsin, and Minnesota, where upward of 60% of wind reports are attributed to QLCSs. Most QLCS wind reports in the central CONUS constitute 20 to 35% of all wind reports (Figure 13e).

### *iii. QLCS-attributable hail*

Severe hail is the smallest threat posed by QLCSs because these storms do not tend to have the intense updrafts characterized by mesocyclones embedded in supercells, which often produce large hail, especially in excess of 2 inches in diameter (Gallus et al. 2008). QLCS hail reports can vary widely on an annual basis, with counts ranging between 500 and 1600 per year (Figure 14a). QLCSs only account for 8% to 15% of total hail reports in any year, with a notable, but slight, downward trend in the QLCS proportion over the period of record (Figure 14a).

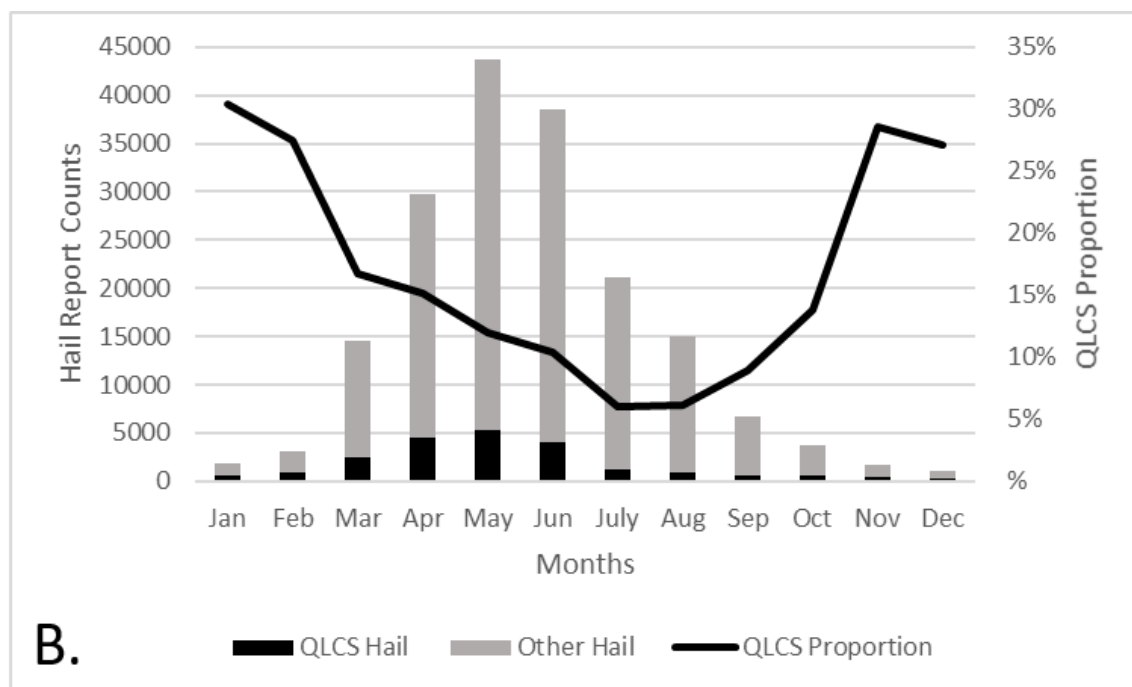
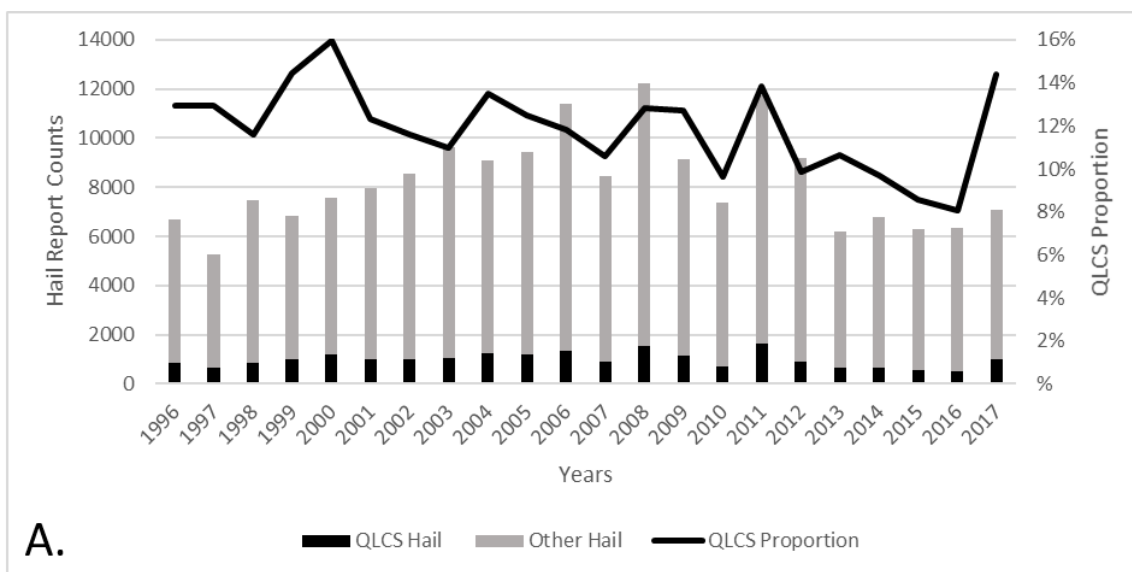


Figure 14. As in Figure 13, but for severe hail reports. Continued on following page.

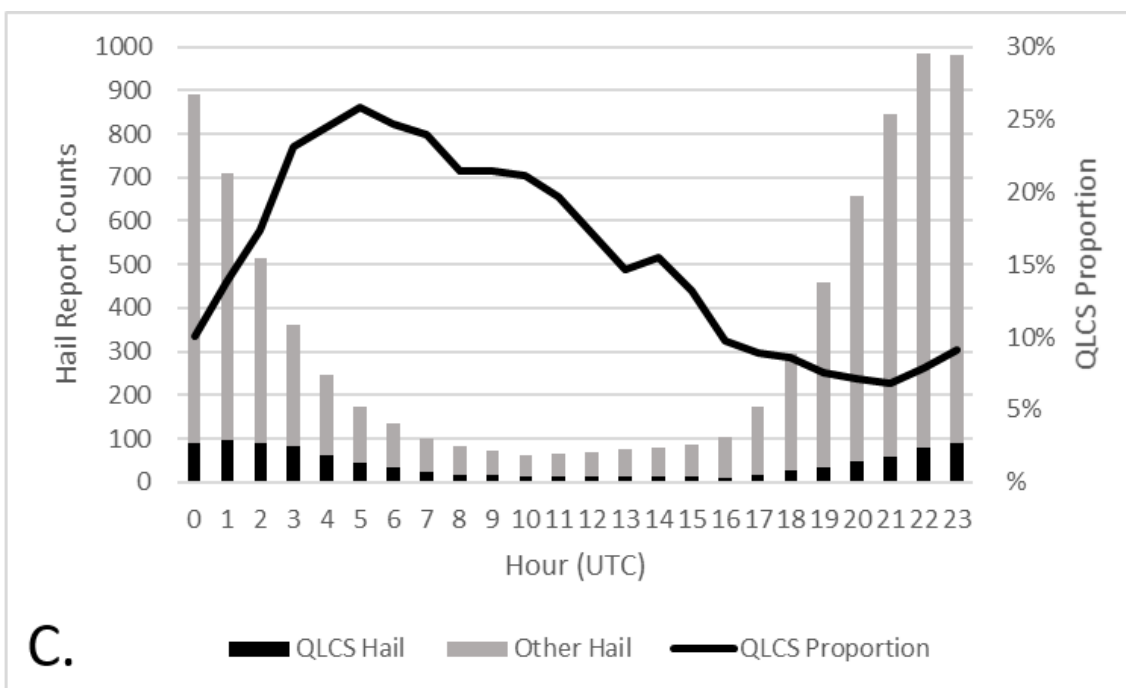


Figure 14. Continued on following page.

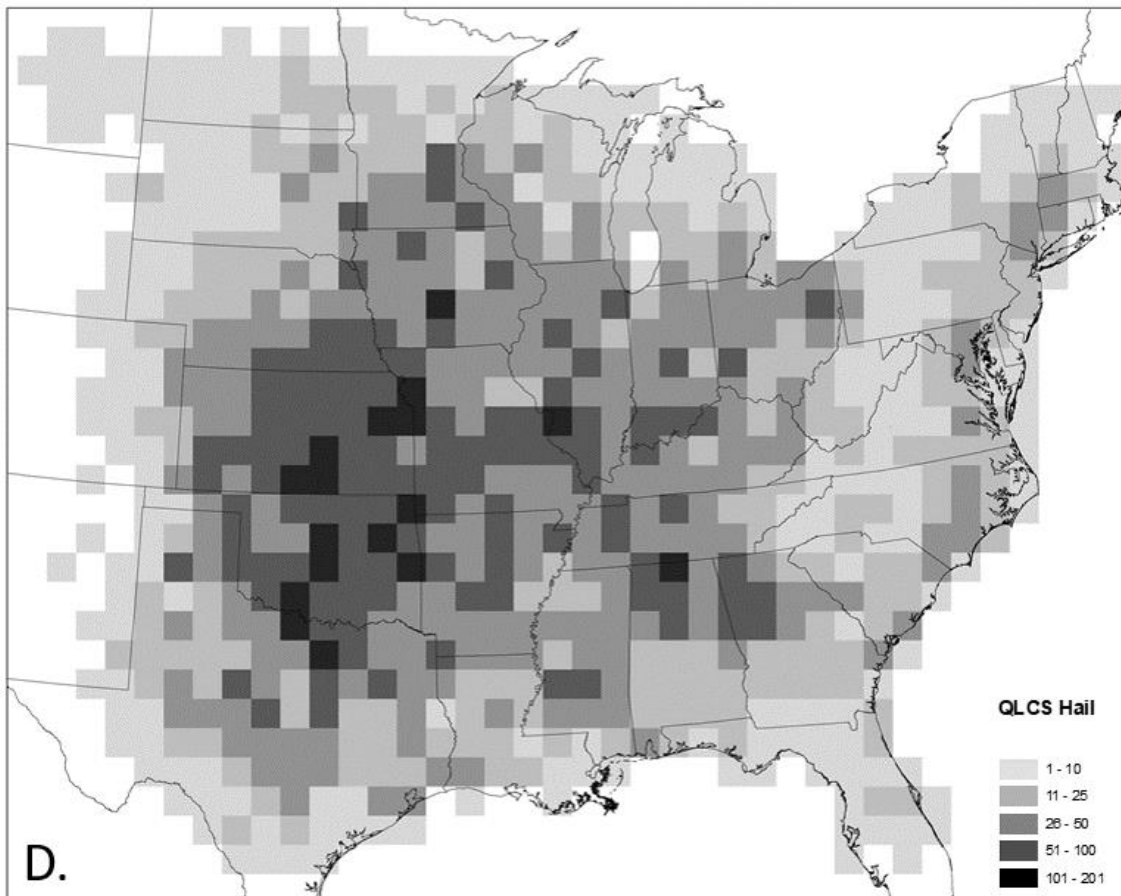


Figure 14. Continued on following page.

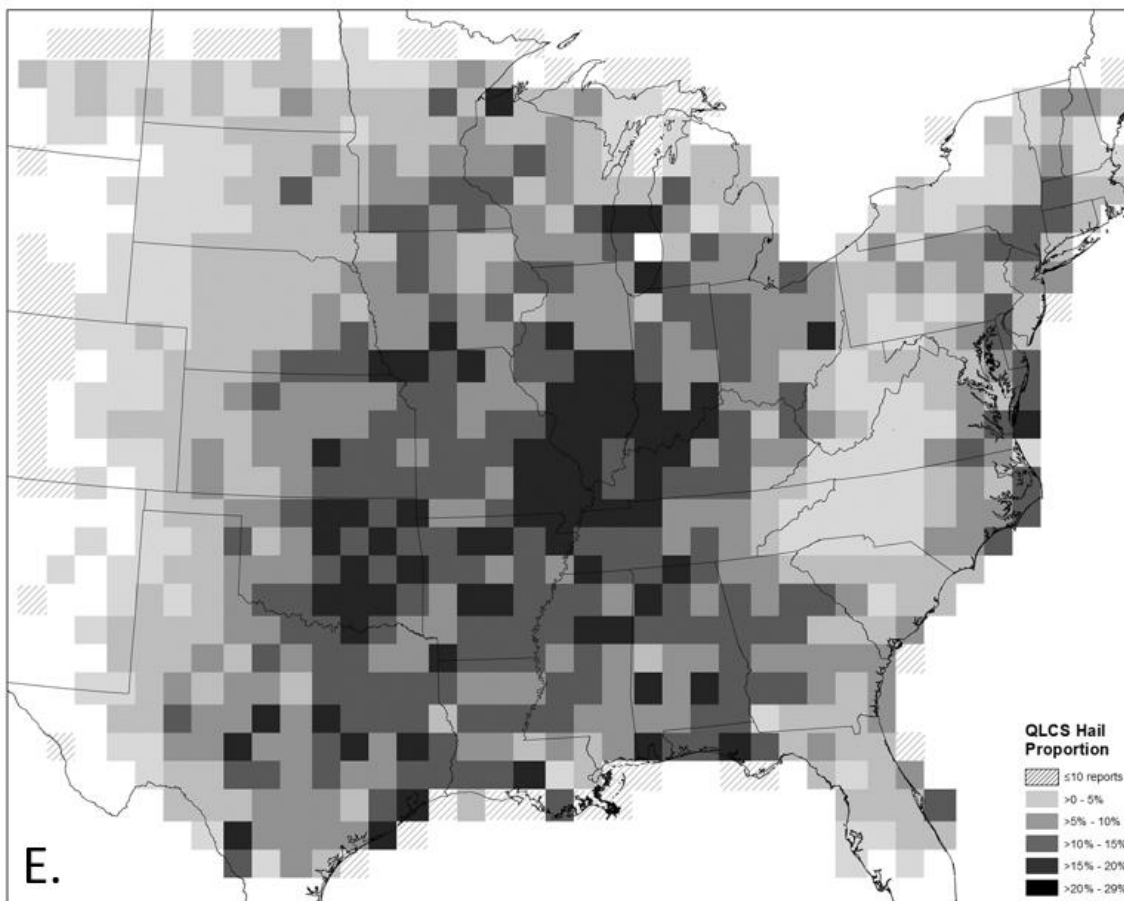


Figure 14.

Monthly, QLCS hail reports are highest in April and May. This mid-spring peak in overall hail counts may be associated with environments more favorable to supercells, which, by their nature, have intense updrafts supportive of large hail. Oftentimes, supercells and/or mesovortices can be embedded in linear convection; this tends to occur in the spring, when shear is elevated in an environment characterized by moderate instability (Gallus et al. 2008). Lines that include these circulations are likely more adept at producing severe hail, which may explain the seasonal peak in April and May. As the number of QLCSs begins to decrease in July, QLCS-

affiliated hail reports reach their minimum proportion of 6%. This proportion of hail events due to QLCSs rises through the fall months, peaking above 30% in January (Figure 14b). QLCS hail reports follow the same diurnal distribution as wind, decreasing during the morning and increasing during the night (Figure 14c). The proportion of reports due to QLCSs differs slightly, however, with a sharper peak above 25% at 5Z that drops below 7% at 21Z. The 5Z proportional maximum occurs in tandem with the daily peak of most QLCS activity both seasonally and spatially (Figure 14c).

Kansas and Oklahoma are the focus of QLCS hail reports, with most areas of these two states experiencing an average of about 2.3 QLCS hail reports per 80 by 80 km cell annually, up to a maximum of 9.1. The frequency of QLCS hail decreases to the east, with 1.2 to 2.3 QLCS hail reports common across Midwest and South grid cells (Figure 14d).

The highest proportions of QLCS-attributable hail are found in Illinois, Missouri, Indiana, and Kentucky, where QLCS wind proportions were also high. However, there is no cluster of higher hail proportions in Iowa, Minnesota, and Wisconsin as there was with wind reports. Smith et al. (2012) found significant hail reports due to supercells to be centered in the Great Plains. Therefore, the proportional maximum in QLCS hail reports found in the Midwest may be due to a relative lack of supercell activity there (Figure 14e).

#### 4. Conclusions

This thesis employed a QLCS-detection algorithm on more than two decades of radar data to generate the first long-term climatology of QLCSs and their affiliated hazards across the CONUS. The research questions posed in this thesis were:

- How are QLCSs spatiotemporally distributed across the conterminous U.S.?
- How do QLCSs vary spatiotemporally across the study period, and have they become more variable?
- What proportion of severe and significant severe storm reports are attributable to the QLCS morphology, and how does this attribution vary spatiotemporally?

QLCSs were found to be most frequent in the east-central U.S., with foci around the Great Plains and Ozark Plateau, and along an axis extending from Illinois and Indiana south to the central Gulf Coast. Over the 22-year study period, QLCSs had high interannual variability, ranging from 101 to 182 events per year. Monthly, QLCSs are most frequent in spring, with activity peaking in June. QLCSs display a distinct diurnal cycle and are primarily late afternoon and overnight phenomena. QLCSs are responsible for an average of 34% of severe wind reports, 12% of severe hail reports, and 23% of tornado reports. These hazards are most frequent in Kentucky and Tennessee, except for QLCS hail, which is more common over eastern Missouri and south-central Illinois. The proportion of storm reports due to QLCS is highest overnight and in the early morning hours, when other storm modes are not as common.

Unlike prior works that have examined short time periods or small spatial domains (Bluestein and Jain 1985, Parker and Johnson 2000, Trapp et al. 2005, Duda and Gallus 2010), this research used a consistent classification procedure on an extensive period of record to reveal the spatiotemporal aspects, including variability, of QLCSs as well as generate an important baseline understanding of the societal impact of these events. This new information will assist in preparation and mitigation of future QLCS hazards in regions most frequently affected by these events.

The process of fine-tuning the algorithm to properly identify QLCSs was one of the greatest challenges encountered during this study. To avoid both underestimation and overestimation of the number of QLCSs that occur, thresholds in the machine learning environment had to be evaluated. Subsequent testing of objective thresholds by the author, as well as Drs. Ashley and Haberlie, produced a robust algorithm that captured most of the QLCS events subjectively identified. The algorithm promotes an efficient method at assessing  $10^6$  radar depictions with consistency in defining events.

Future work should continue to expand on the time period used in this study and investigate if there are any changes to the findings presented here over longer time scales. Examination of the synoptic scale environments associated with QLCSs across different seasons will help forecasters know when they may expect QLCS activity throughout the year. Additional research should seek to understand the mortality, morbidity, and monetary costs QLCS hazards impose on society, whether from wind, hail, tornadoes, or flooding. This thesis has revealed the quantity and distribution of QLCS hazards, but the totality of the economic costs and societal impacts (e.g., death and injuries) were not addressed. Flooding is another important QLCS-related hazard that has been discussed at length in many studies (Pettet and Johnson 2003,

Schumacher and Johnson 2005, 2006, Gallus et al. 2008, Duda and Gallus 2010) but was not analyzed here due to its exclusion from the SVRGIS database. Finally, by assessing the probability of detection and false alarm ratio of QLCS tornadoes (i.e., Anderson-Frey et al. 2016), along with this new insight into QLCS climatology, operational meteorologists can begin to make improvements. Knowing the answers to these questions, in addition to the knowledge gained in this thesis, will improve forecasting techniques and help to educate the public on the risks they face.

## REFERENCES

- Anderson, C. J., and R.W. Arritt, 1998: Mesoscale Convective Complexes and Persistent Elongated Convective Systems over the U.S. during 1992 and 1993. *Mon. Wea. Rev.*, **126**, 578-599, [https://doi.org/10.1175/1520-0493\(1998\)126<0578:MCCAPE>2.0.CO;2](https://doi.org/10.1175/1520-0493(1998)126<0578:MCCAPE>2.0.CO;2)
- Anderson-Frey, A.K., Y.P. Richardson, A.R. Dean, R.L. Thompson, and B.T. Smith, 2016: Investigation of Near-Storm Environments for Tornado Events and Warnings. *Wea. Forecasting*, **31**, 1771–1790, <https://doi.org/10.1175/WAF-D-16-0046.1>
- Arritt, R. W., T. D. Rink, M. Segal, D. P. Todey, C. A. Clark, M. J. Mitchell, and K. M. Labas, 1997: The Great Plains low-level jet during the warm season of 1993. *Mon. Wea. Rev.*, **125**, 2176–2192, [https://doi.org/10.1175/1520-0493\(1997\)125<2176:TGPLLJ>2.0.CO;2](https://doi.org/10.1175/1520-0493(1997)125<2176:TGPLLJ>2.0.CO;2).
- Ashley, W.S., 2007: Spatial and Temporal Analysis of Tornado Fatalities in the U.S.: 1880-2005. *Wea. Forecasting*, **22**, 1214-1228, <https://doi.org/10.1175/2007WAF2007004.1>
- Ashley, S.T., and W.S. Ashley, 2008: The storm morphology of deadly flooding events in the U.S. *Int. J. Climatol.*, **28**, 493-503, <https://doi.org/10.1002/joc.1554>
- Ashley, W.S., and T.L. Mote, 2005: Derecho Hazards in the United States. *Bull. Amer. Meteor. Soc.*, **86**, 1577-1592, <https://doi.org/10.1175/BAMS-86-11-1577>
- Ashley, W.S., T.L. Mote, P.G. Dixon, S.L. Trotter, E.J. Powell, J.D. Durkee, and A.J. Grundstein, 2003: Distribution of Mesoscale Convective Complex Rainfall in the United States. *Mon. Wea. Rev.*, **131**, 3003–3017, [https://doi.org/10.1175/1520-0493\(2003\)131<3003:DOMCCR>2.0.CO;2](https://doi.org/10.1175/1520-0493(2003)131<3003:DOMCCR>2.0.CO;2)
- Ashley, W.S., A.J. Krmenc, and R. Schwantes, 2008: Vulnerability due to Nocturnal Tornadoes. *Wea. Forecasting*, **23**, 795-807, <https://doi.org/10.1175/2008WAF2222132.1>
- Ashley, W.S. and S.M. Strader, 2016: Recipe for Disaster: How the Dynamic Ingredients of Risk and Exposure Are Changing the Tornado Disaster Landscape. *Bull. Amer. Meteor. Soc.*, **97**, 767–786, <https://doi.org/10.1175/BAMS-D-15-00150.1>

- Atkins, N. T., and M. St. Laurent, 2009: Bow echo mesovortices. Part II: Their Genesis. *Mon. Wea. Rev.*, **137**, 1514–1532, <https://doi.org/10.1175/2008MWR2650.1>
- Bentley, M. L. and T.L. Mote, 1998: A Climatology of Derecho-Producing Mesoscale Convective Systems in the Central and Eastern U.S., 1986–95. Part I: Temporal and Spatial Distribution. *Bull. Amer. Meteor. Society*, **79**, 2527-2540  
[https://doi.org/10.1175/1520-0477\(1998\)079<2527:ACODPM>2.0.CO;2](https://doi.org/10.1175/1520-0477(1998)079<2527:ACODPM>2.0.CO;2)
- Black, A.W., and W.S. Ashley, 2011: The Relationship between Tornadic and Nontornadic Convective Wind Fatalities and Warnings. *Wea. Climate Soc.*, **3**, 31-47, <https://doi.org/10.1175/2010WCAS1094.1>
- Bluestein, H.B., 2013: *Severe Convective Storms and Tornadoes: Observations and Dynamics*, Praxis Publishing, 456 pp.
- Bluestein, H.B., and M.H. Jain, 1985: Formation of Mesoscale Lines of Precipitation: Severe Squall Lines in Oklahoma during the Spring. *J. Atmos. Sci.*, **42**, 1711-1732,  
[https://doi.org/10.1175/1520-0469\(1985\)042<1711:FOMLOP>2.0.CO;2](https://doi.org/10.1175/1520-0469(1985)042<1711:FOMLOP>2.0.CO;2)
- Brooks, H. E., G. W. Carbin, and P. T. Marsh, 2014: Increased variability of tornado occurrence in the United States. *Science*, **346**, 349–352, <https://doi.org/10.1126/science.1257460>.
- Brooks, H.E., C.A. Doswell, and M.P. Kay, 2003: Climatological Estimates of Local Daily Tornado Probability for the United States. *Wea. Forecasting*, **18**, 626–640,  
[https://doi.org/10.1175/1520-0434\(2003\)018<0626:CEOLDT>2.0.CO;2](https://doi.org/10.1175/1520-0434(2003)018<0626:CEOLDT>2.0.CO;2)
- Brotzge, J.A., S.E. Nelson, R.L. Thompson, and B.T. Smith, 2013: Tornado Probability of Detection and Lead Time as a Function of Convective Mode and Environmental Parameters. *Wea. Forecasting*, **28**, 1261–1276, <https://doi.org/10.1175/WAF-D-12-00119.1>
- Campbell, M.A., A.E. Cohen, M.C. Coniglio, A.R. Dean, S.F. Corfidi, S.J. Corfidi, and C.M. Mead, 2017: Structure and Motion of Severe-Wind-Producing Mesoscale Convective Systems and Derechos in Relation to the Mean Wind. *Wea. Forecasting*, **32**, 423–439, <https://doi.org/10.1175/WAF-D-16-0060.1>
- Coniglio, M.C., and D.J. Stensrud, 2004: Interpreting the Climatology of Derechos. *Wea. Forecasting*, **19**, 595-605, [https://doi.org/10.1175/1520-0434\(2004\)019<0595:ITCOD>2.0.CO;2](https://doi.org/10.1175/1520-0434(2004)019<0595:ITCOD>2.0.CO;2)
- Corfidi, S.F., M.C. Coniglio, A.E. Cohen, and C.M. Mead, 2016: A Proposed Revision to the Definition of “Derecho”. *Bull. Amer. Meteor. Soc.*, **97**, 935–949,  
<https://doi.org/10.1175/BAMS-D-14-00254.1>

- Cotton, W. C., M-S. Lin, R. L. McAnelly, and C. J. Tremback, 1989: A composite model of mesoscale convective complexes. *Mon. Wea. Rev.*, **117**, 765–783, [https://doi.org/10.1175/1520-0493\(1989\)117<0765:ACMOMC>2.0.CO;2](https://doi.org/10.1175/1520-0493(1989)117<0765:ACMOMC>2.0.CO;2)
- Dieleman, S., Willett, K. W. & Dambre, J., 2015: Rotation-invariant convolutional neural networks for galaxy morphology prediction. *Mon. Not. R. Astron. Soc.*, **450**, 1441–1459.
- Doswell, C.A., H.E. Brooks, and M.P. Kay, 2005: Climatological Estimates of Daily Local Nontornadic Severe Thunderstorm Probability for the United States. *Wea. Forecasting*, **20**, 577–595, <https://doi.org/10.1175/WAF866.1>
- Doswell, C.A., H.E. Brooks, and R.A. Maddox, 1996: Flash Flood Forecasting: An Ingredients-Based Methodology. *Wea. Forecasting*, **11**, 560–581, [https://doi.org/10.1175/1520-0434\(1996\)011<0560:FFFAIB>2.0.CO;2](https://doi.org/10.1175/1520-0434(1996)011<0560:FFFAIB>2.0.CO;2) .
- Doswell, C.A. III, and D.W. Burgess, 1988: On Some Issues of United States Tornado Climatology. *Mon. Wea. Rev.*, **116**, 495–501, doi: 10.1175/1520-0493(1988)116<0495:OSIOUS>2.0.CO;2
- Duda, J. D., and W.A. Gallus, 2010: Spring and Summer Midwestern Severe Weather Reports in Supercells Compared to Other Morphologies. *Wea. Forecasting*, **25**, 190-206, <https://doi.org/10.1175/2009WAF2222338.1>
- Edwards, R., J.T. Allen, and G.W. Carbin, 2018: Reliability and Climatological Impacts of Convective Wind Estimations. *J. Appl. Meteor. Climatol.*, **57**, 1825–1845, <https://doi.org/10.1175/JAMC-D-17-0306.1>
- Eichler, T. and W. Higgins, 2006: Climatology and ENSO-Related Variability of North American Extratropical Cyclone Activity. *J. Climate*, **19**, 2076–2093, <https://doi.org/10.1175/JCLI3725.1>
- Ferreira, R.N., L. Hall, and T.M. Rickenbach, 2013: A Climatology of the Structure, Evolution, and Propagation of Midlatitude Cyclones in the Southeast United States. *J. Climate*, **26**, 8406–8421, <https://doi.org/10.1175/JCLI-D-12-00657.1>
- Fritsch, J.M., and G.S. Forbes, 2001: Mesoscale Convective Systems. *Severe Convective Storms*, C. Doswell, Ed., American Meteorological Society, 323-357.
- Fritsch, J.M., R.J. Kane, and C.R. Chelius, 1986: The Contribution of Mesoscale Convective Weather Systems to the Warm-Season Precipitation in the United States. *J. Climate Appl. Meteor.*, **25**, 1333–1345, [https://doi.org/10.1175/1520-0450\(1986\)025<1333:TCOMCW>2.0.CO;2](https://doi.org/10.1175/1520-0450(1986)025<1333:TCOMCW>2.0.CO;2)

- Fujita, T., 1978: Manual of downburst identification for project NIMROD. Satellite and Mesometeorology Res. Pap. No. 156, University of Chicago, Dept. of Geophysical Sciences, pp. 104.
- Gagne, D. J., Haupt S. E., and Nychka D. W. (2017) Evaluation of Deep Learning Representations of Spatial Storm Data. In *AGU Fall Meeting Abstracts*.
- Gallus, W.A., N.A. Snook, and E.V. Johnson, 2008: Spring and Summer Severe Weather Reports over the Midwest as a Function of Convective Mode: A Preliminary Study. *Wea. Forecasting*, **23**, 101–113, <https://doi.org/10.1175/2007WAF2006120.1>
- Gensini, V. A., and W. S. Ashley, 2011: Climatology of potentially severe convective environments from North American regional reanalysis. *Electronic J. Severe Storms Meteor* 6 (8), 1–40.
- Geerts, B., 1998: Mesoscale Convective Systems in the Southeast United States during 1994–95: A Survey. *Wea. Forecasting*, **13**, 860–869, [https://doi.org/10.1175/1520-0434\(1998\)013<0860:MCSITS>2.0.CO;2](https://doi.org/10.1175/1520-0434(1998)013<0860:MCSITS>2.0.CO;2)
- Geerts, B., D. Parsons, C.L. Ziegler, T.M. Weckwerth, M.I. Biggerstaff, R.D. Clark, M.C. Coniglio, B.B. Demoz, R.A. Ferrare, W.A. Gallus, K. Haghi, J.M. Hanesiak, P.M. Klein, K.R. Knupp, K. Kosiba, G.M. McFarquhar, J.A. Moore, A.R. Nehrir, M.D. Parker, J.O. Pinto, R.M. Rauber, R.S. Schumacher, D.D. Turner, Q. Wang, X. Wang, Z. Wang, and J. Wurman, 2017: The 2015 Plains Elevated Convection at Night Field Project. *Bull. Amer. Meteor. Soc.*, **98**, 767–786, <https://doi.org/10.1175/BAMS-D-15-00257.1>
- Grams, J.S., R.L. Thompson, D.V. Snively, J.A. Prentice, G.M. Hodges, and L.J. Reames, 2012: A Climatology and Comparison of Parameters for Significant Tornado Events in the United States. *Wea. Forecasting*, **27**, 106–123, <https://doi.org/10.1175/WAF-D-11-00008.1>
- Guastini, C.T. and L.F. Bosart, 2016: Analysis of a Progressive Derecho Climatology and Associated Formation Environments. *Mon. Wea. Rev.*, **144**, 1363–1382, <https://doi.org/10.1175/MWR-D-15-0256.1>
- Haberlie, A., and W.S. Ashley, 2018a: Climatological Representation of Mesoscale Convective Systems in a Dynamically Downscaled Climate Simulation. *Int. J. Climatol.*
- Haberlie, A., and W.S. Ashley, 2018b: A Method for Identifying Midlatitude Mesoscale Convective Systems in Radar Mosaics. Part I: Segmentation and Classification. *J. Appl. Meteor. Climatol.*, **57**, 1575–1598, <https://doi.org/10.1175/JAMC-D-17-0293.1>
- Haberlie, A., and W.S. Ashley, 2018c: A Method for Identifying Midlatitude Mesoscale Convective Systems in Radar Mosaics. Part II: Tracking. *J. Appl. Meteor. Climatol.*, **57**, 1599–1621, <https://doi.org/10.1175/JAMC-D-17-0294.1>

- Haberlie, A. M., and W. S. Ashley, 2019: A radar-based climatology of mesoscale convective systems in the United States. *Journal of Climate*. doi: JCLI-D-18-0559.1
- Heideman, K.F., and Fritsch, J.M., 1984: A quantitative evaluation the warm-season QPF problem. *Preprints Tenth Conf. on Weather Forecasting and Analysis*, Clearwater Beach, Amer. Meteor. Soc. 57-64.
- Higgins, R. W., Y. Yao, E. S. Yarosh, J. Eo Janowiak, and K. C. Mo, 1997: Influence of the Great Plains low-level jet on summertime precipitation and moisture transport over the central United States. *J. Climate*, **10**, 481-507, [https://doi.org/10.1175/1520-0442\(1997\)010<0481:IOTGPL>2.0.CO;2](https://doi.org/10.1175/1520-0442(1997)010<0481:IOTGPL>2.0.CO;2)
- Hilgendorf, E.R. and R.H. Johnson, 1998: A Study of the Evolution of Mesoscale Convective Systems Using WSR-88D Data. *Wea. Forecasting*, **13**, 437–452, [https://doi.org/10.1175/1520-0434\(1998\)013<0437:ASOTEO>2.0.CO;2](https://doi.org/10.1175/1520-0434(1998)013<0437:ASOTEO>2.0.CO;2)
- Houze, R.A., 2004: Mesoscale convective systems. *Reviews of Geophysics*, **42**, RG4003.
- Houze, R.A., 2018: 100 Years of Research on Mesoscale Convective Systems. *Meteorological Monographs*, **59**, 17.1–17.54, <https://doi.org/10.1175/AMSMONOGRAPHS-D-18-0001.1>
- Jirak, I.L., W.R. Cotton, and R.L. McAnelly, 2003: Satellite and Radar Survey of Mesoscale Convective System Development. *Mon. Wea. Rev.*, **131**, 2428–2449, [https://doi.org/10.1175/1520-0493\(2003\)131<2428:SARSOM>2.0.CO;2](https://doi.org/10.1175/1520-0493(2003)131<2428:SARSOM>2.0.CO;2)
- Johns, R.H. and W.D. Hirt, 1987: Derechos: Widespread Convectively Induced Windstorms. *Wea. Forecasting*, **2**, 32–49, [https://doi.org/10.1175/1520-0434\(1987\)002<0032:DWCIW>2.0.CO;2](https://doi.org/10.1175/1520-0434(1987)002<0032:DWCIW>2.0.CO;2)
- Kis, A.K. and J.M. Straka, 2010: Nocturnal Tornado Climatology. *Wea. Forecasting*, **25**, 545–561, <https://doi.org/10.1175/2009WAF2222294.1>
- Krizhevsky, A., Sutskever, I. & Hinton, G. E., 2012: Imagenet classification with deep convolutional neural networks. In *Advances in neural information processing systems*, 1097–1105.
- Laing, A.G., and Fritsch, J.M., 1993a: Mesoscale Convective Complexes in Africa. *Mon. Wea. Rev.*, **121**, 2254–2263, [https://doi.org/10.1175/1520-0493\(1993\)121<2254:MCCIA>2.0.CO;2](https://doi.org/10.1175/1520-0493(1993)121<2254:MCCIA>2.0.CO;2)
- Laing, A.G., and Fritsch, J.M., 1993b: Mesoscale Convective Complexes over the Indian Monsoon Region. *J. Climate*, **6**, 911–919, [https://doi.org/10.1175/1520-0442\(1993\)006<0911:MCCOTI>2.0.CO;2](https://doi.org/10.1175/1520-0442(1993)006<0911:MCCOTI>2.0.CO;2)

- Lericos, T. P., H. E. Fuelberg, A. I. Watson, and R. L. Holle, 2002: Warm season lightning distributions over the Florida peninsula as related to synoptic patterns. *Wea. Forecasting*, **17**, 83–98, [https://doi.org/10.1175/1520-0434\(2002\)017<0083:WSLDOT>2.0.CO;2](https://doi.org/10.1175/1520-0434(2002)017<0083:WSLDOT>2.0.CO;2)
- Lombardo, K.A. and B.A. Colle, 2010: The Spatial and Temporal Distribution of Organized Convective Structures over the Northeast and Their Ambient Conditions. *Mon. Wea. Rev.*, **138**, 4456–4474, <https://doi.org/10.1175/2010MWR3463.1>
- Maddox, R.A., 1980: Mesoscale Convective Complexes. *Bull. Amer. Meteor. Soc.*, **61**, 1375-1387.
- Maddox, R.A., 1983: Large-Scale Meteorological Conditions Associated with Midlatitude, Mesoscale Convective Complexes. *Mon. Wea. Rev.*, **111**, 1475–1493, [https://doi.org/10.1175/1520-0493\(1983\)111<1475:LSMCAW>2.0.CO;2](https://doi.org/10.1175/1520-0493(1983)111<1475:LSMCAW>2.0.CO;2)
- Markowski, P., and Richardson, Y., 2010: *Mesoscale Meteorology in Midlatitudes*. Wiley-Blackwell, 430 pp.
- Miller, D. and J.M. Fritsch, 1991: Mesoscale Convective Complexes in the Western Pacific Region. *Mon. Wea. Rev.*, **119**, 2978–2992, [https://doi.org/10.1175/1520-0493\(1991\)119<2978:MCCITW>2.0.CO;2](https://doi.org/10.1175/1520-0493(1991)119<2978:MCCITW>2.0.CO;2)
- National Weather Service, 2015: Weather Prediction Center. Accessed 23 October 2018 [Available online at <https://www.wpc.ncep.noaa.gov>]
- NOAA, 2017: Storm Prediction Center. Accessed 10 April 2017. [Available online at <http://www.spc.noaa.gov>]
- Orlanski, I., 1975: A Rational Subdivision of Scales for Atmospheric Processes. *Bull. Amer. Meteor. Soc.*, **56**, 527-530.
- Parker, M.D. and D.A. Ahijevych, 2007: Convective Episodes in the East-Central United States. *Mon. Wea. Rev.*, **135**, 3707–3727, <https://doi.org/10.1175/2007MWR2098.1>
- Parker, M.D. and R.H. Johnson, 2000: Organizational Modes of Midlatitude Mesoscale Convective Systems. *Mon. Wea. Rev.*, **128**, 3413–3436, [https://doi.org/10.1175/1520-0493\(2001\)129<3413:OMOMMC>2.0.CO;2](https://doi.org/10.1175/1520-0493(2001)129<3413:OMOMMC>2.0.CO;2)
- Parker, M.D. and J.C. Knievel, 2005: Do Meteorologists Suppress Thunderstorms?: Radar-Derived Statistics and the Behavior of Moist Convection. *Bull. Amer. Meteor. Soc.*, **86**, 341–358, <https://doi.org/10.1175/BAMS-86-3-341>

- Pettet, C.R. and R.H. Johnson, 2003: Airflow and Precipitation Structure of Two Leading Stratiform Mesoscale Convective Systems Determined from Operational Datasets. *Wea. Forecasting*, **18**, 685–699, [https://doi.org/10.1175/1520-0434\(2003\)018<0685:AAPSOT>2.0.CO;2](https://doi.org/10.1175/1520-0434(2003)018<0685:AAPSOT>2.0.CO;2)
- Pitchford, K.L. and J. London, 1962: The Low-Level Jet as Related to Nocturnal Thunderstorms over Midwest United States. *J. Appl. Meteor.*, **1**, 43–47, [https://doi.org/10.1175/1520-0450\(1962\)001<0043:TLLJAR>2.0.CO;2](https://doi.org/10.1175/1520-0450(1962)001<0043:TLLJAR>2.0.CO;2)
- Pu, B., and R. E. Dickinson, 2014: Diurnal spatial variability of Great Plains summer precipitation related to the dynamics of the low-level jet. *J. Atmos. Sci.*, **71**, 1807–1817, <https://doi.org/10.1175/JAS-D-13-0243.1>
- Schoen, J.M. and W.S. Ashley, 2011: A Climatology of Fatal Convective Wind Events by Storm Type. *Wea. Forecasting*, **26**, 109–121, <https://doi.org/10.1175/2010WAF2222428.1>
- Schultz, D.M., 2005: A Review of Cold Fronts with Prefrontal Troughs and Wind Shifts. *Mon. Wea. Rev.*, **133**, 2449–2472, <https://doi.org/10.1175/MWR2987.1>
- Schultz, D.M. and W.J. Steenburgh, 1999: The Formation of a Forward-Tilting Cold Front with Multiple Cloud Bands during Superstorm 1993. *Mon. Wea. Rev.*, **127**, 1108–1124, [https://doi.org/10.1175/1520-0493\(1999\)127<1108:TFOAFT>2.0.CO;2](https://doi.org/10.1175/1520-0493(1999)127<1108:TFOAFT>2.0.CO;2)
- Schumacher, R.S. and R.H. Johnson, 2005: Organization and Environmental Properties of Extreme-Rain-Producing Mesoscale Convective Systems. *Mon. Wea. Rev.*, **133**, 961–976, <https://doi.org/10.1175/MWR2899.1>
- Schumacher, R.S. and R.H. Johnson, 2006: Characteristics of U.S. Extreme Rain Events during 1999–2003. *Wea. Forecasting*, **21**, 69–85, <https://doi.org/10.1175/WAF900.1>
- Skow, K.D. and C. Cogil, 2017: A High-Resolution Aerial Survey and Radar Analysis of Quasi-Linear Convective System Surface Vortex Damage Paths from 31 August 2014. *Wea. Forecasting*, **32**, 441–467, <https://doi.org/10.1175/WAF-D-16-0136.1>
- Smith, B.T., T.E. Castellanos, A.C. Winters, C.M. Mead, A.R. Dean, and R.L. Thompson, 2013: Measured Severe Convective Wind Climatology and Associated Convective Modes of Thunderstorms in the Contiguous United States, 2003–09. *Wea. Forecasting*, **28**, 229–236, <https://doi.org/10.1175/WAF-D-12-00096.1>
- Smith, B.T., R.L. Thompson, J.S. Grams, C. Broyles, and H.E. Brooks, 2012: Convective Modes for Significant Severe Thunderstorms in the Contiguous United States. Part I: Storm Classification and Climatology. *Wea. Forecasting*, **27**, 1114–1135, <https://doi.org/10.1175/WAF-D-11-00115.1>

- Stevenson, S.N. and R.S. Schumacher, 2014: A 10-Year Survey of Extreme Rainfall Events in the Central and Eastern United States Using Gridded Multisensor Precipitation Analyses. *Mon. Wea. Rev.*, **142**, 3147–3162, <https://doi.org/10.1175/MWR-D-13-00345.1>
- Trapp, R.J., S.A. Tessendorf, E.S. Godfrey, and H.E. Brooks, 2005: Tornadoes from Squall Lines and Bow Echoes. Part I: Climatological Distribution. *Wea. Forecasting*, **20**, 23–34, <https://doi.org/10.1175/WAF-835.1>
- Trapp, R.J. and M.L. Weisman, 2003: Low-Level Mesovortices within Squall Lines and Bow Echoes. Part II: Their Genesis and Implications. *Mon. Wea. Rev.*, **131**, 2804–2823, [https://doi.org/10.1175/1520-0493\(2003\)131<2804:LMWSLA>2.0.CO;2](https://doi.org/10.1175/1520-0493(2003)131<2804:LMWSLA>2.0.CO;2)
- Trapp, R.J., D.M. Wheatley, N.T. Atkins, R.W. Przybylinski, and R. Wolf, 2006: Buyer Beware: Some Words of Caution on the Use of Severe Wind Reports in Postevent Assessment and Research. *Wea. Forecasting*, **21**, 408–415, <https://doi.org/10.1175/WAF925.1>
- Trier, S.B., C.A. Davis, D.A. Ahijevych, M.L. Weisman, and G.H. Bryan, 2006: Mechanisms Supporting Long-Lived Episodes of Propagating Nocturnal Convection within a 7-Day WRF Model Simulation. *J. Atmos. Sci.*, **63**, 2437–2461, <https://doi.org/10.1175/JAS3768.1>
- Tuttle, J.D. and C.A. Davis, 2006: Corridors of Warm Season Precipitation in the Central United States. *Mon. Wea. Rev.*, **134**, 2297–2317, <https://doi.org/10.1175/MWR3188.1>
- University Corporation for Atmospheric Research, 2017: Image Archive Meteorological case study selection kit. Accessed 30 September 2017, <http://www2.mmm.ucar.edu/imagearchive/>
- Velasco, I., and Fritsch, J.M., 1987: Mesoscale convective complexes in the Americas. *Journal of Geophysical Research*, **92**, 9591–9613.
- Weisman, M.L. and C.A. Davis, 1998: Mechanisms for the Generation of Mesoscale Vortices within Quasi-Linear Convective Systems. *J. Atmos. Sci.*, **55**, 2603–2622, [https://doi.org/10.1175/1520-0469\(1998\)055<2603:MFTGOM>2.0.CO;2](https://doi.org/10.1175/1520-0469(1998)055<2603:MFTGOM>2.0.CO;2)
- Weiss, S. J., J. A. Hart, and P. R. Janish, 2002: An examination of severe thunderstorm wind report climatology: 1970–1999. *Preprints, 21st Conf. on Severe Local Storms*, San Antonio, TX, Amer. Meteor. Soc., 446–449.
- Zipser, E. J., 1982: Use of a conceptual model of the life cycle of mesoscale convective systems to improve very-short-range forecasts. *Nowcasting*, K. Browning, Ed., Academic Press, 191–204.